

AD-A123 580

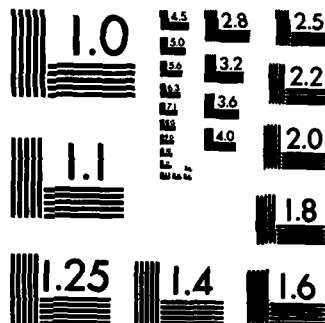
PHOTOEMISSION OF XE AND KR ADSORBED ON THE W(110) PLANE 1/1
(U) CHICAGO UNIV IL JAMES FRANCK INST R OPILA ET AL.
1977 N00014-77-C-0018

UNCLASSIFIED

F/G 7/4

NL

END
FORMED
BY
DATE



MICROCOPY RESOLUTION TEST CHART
NATIONAL BUREAU OF STANDARDS-1963-A

PHOTOEMISSION OF Xe and Kr ADSORBED ON THE W(110) PLANE

R. Opila* and R. Gomer
Department of Chemistry and
The James Franck Institute
The University of Chicago
5640 South Ellis Avenue
Chicago, IL 60637

ABSTRACT

The UPS and XPS spectra of Xe adsorbed on clean, O, CO, and Xe covered W(110) surfaces and the UPS spectrum of Kr on clean and O covered W(110) surfaces have been investigated. On clean W, Xe and Kr show a splitting of the $5p_{3/2}$ and $4p_{3/2}$ hole states respectively. For Xe the coverage dependence of this splitting was investigated in detail; neither the positions or the intensity ratio of the substates are coverage dependent for $\theta > 0.04$, suggesting that splitting is due to differences in the image interaction of the $m_j = \pm 3/2$ and $m_j = \pm 1/2$ components. For Xe equal shifts, relative to vacuum, of ~ 1.0 eV were observed for 5p, 4d, and 3d levels, suggesting that initial state effects are small. Image interaction for Xe and Kr on clean W could best be fitted by assuming an increase, rather than a decrease in the effective hole-image separation from the nominal value, suggesting that the image plane is moved back into the metal by a screening length. For Xe adsorbed on Xe/W(110), or on virgin-CO/W(110) polarization of the intermediate layers was found to contribute significantly to relaxation. Coadsorbed oxygen broadened Xe 5p and Kr 4p peaks. There was an almost linear relation between O 2p UPS intensity at the energies of the various peaks and the amounts of broadening, suggesting that the latter results from resonance neutralization by electrons from the O 2p states.

*Present Address: Bell Laboratories
Holmdel, NJ 07733

This document has been approved
for public release and sale; its
distribution is unlimited.

62 12 10 039

1. INTRODUCTION

Photoemission from inert gases adsorbed on metal surfaces is interesting because adsorption is very weak so that initial state effects are either small or readily understood. Thus changes from the gas phase spectra provide a very direct probe of final state effects. A number of effects have been reported. Most notably, for Xe adsorption the $5p_{3/2}$ hole state is split into 2 substates. Some workers find this splitting to be coverage dependent and ascribe it to Xe-Xe interactions, [1,2] while others do not find such a dependence and attribute it to Xe surface effects [3]. Some attempts have also been made to correlate the level positions with substrate work function. Ertl and coworkers [4-7] find that for clean surfaces shifts relative to the Fermi energy can be explained by assuming that Xe levels are pinned to the vacuum with relaxation shifts differing little from metal to metal. However, shifts induced by Xe coverage changes do not correspond fully with the work function decrements resulting from Xe adsorption [8]. Kaundl et al. [9] have also looked at level shifts in higher adsorbate layers.

→ In this paper we report results of UPS and XPS studies of Xe adsorbed on clean, Xe covered, oxygen covered, and CO covered W(110) surfaces and also of Kr on clean and oxygen covered surfaces. In particular, we have examined the coverage dependence of the Xe $5p_{3/2}$ splitting on clean and oxygen covered surfaces, the broadening and shifts resulting from adsorption on oxygen and CO precovered surfaces and the changes in intensity caused by these conditions.

2. EXPERIMENTAL

The apparatus used in these experiments has been described previously [10]. For the X-ray photoemission experiments Mg K α ($h\nu = 1253.6$ eV) radiation was used; for the ultraviolet photoemission experiments the light source was a He resonance lamp providing 21.22 eV and 40.8 eV photons. A cylindrical mirror

analyzer (CMA) was used in the retarding mode to detect the energy of the photoelectrons. The electron multiplier pulses passed through a discriminator and amplifier to a digital counter interfaced to a DEC MINC-11 computer. The retarding voltage provided by digital-to-analog converters (DAC's) interfaced to the computer was incremented after each counting period by incrementing the DAC's. The retarding voltage was monitored by a digital voltmeter; the computer could correct voltage drifts by monitoring the digital voltmeter and adjusting the DAC's accordingly. A typical X-ray spectrum covered 30 volts in increments of 0.1 volt, with a counting period of 10 seconds per step. The pass energy of the CMA was 50 volts, with a CMA resolution of 800 meV. For UPS, the pass energy was either 10 or 15 volts with CMA resolutions of 160 or 240 meV, respectively. In all cases the spectrum was taken in less than one hour in order to maintain an uncontaminated surface. Occasionally, in order to improve the signal to noise ratio, several spectra taken under identical conditions were added.

For UPS spectra the energy differences relative to the Fermi edge E_F could be obtained with an accuracy of 30 meV, and energies were measured relative to E_F . In the case of XPS spectra this procedure is much less accurate, since the high kinetic energy edge of the electron distribution is not as well defined. Energies were therefore measured by determining the collector (i.e. analyzer) effective work function. This was done by using He I, 21.2 eV radiation and measuring the battery voltage V_0 between target and analyzer at which the highest energy electrons were just rejected. The collector work function ϕ_c is then $\phi_c = 21.2 - V_0$, since with no bias, target and collector Fermi levels coincide. This measurement was carried out within a day of XPS measurements, so that no change in ϕ_c occurred. Energies of XPS electrons could then be related to the collector vacuum (or Fermi level) by using this value of ϕ_c and $h\nu$. ϕ_c was found to be 5.25 - 5.26 eV without significant changes over at least 6 months.



Letter on file

A

Mg K α radiation consists of a doublet at energies of 1253.7 eV and 1253.4 eV, in the intensity ratio 2:1. A computer simulation was carried out in which a level of Gaussian or Lorentzian shape with FWHM = 1 eV was convoluted with a doublet, assumed to consist of two sharp lines at the energies and with the intensities of the Mg K α doublet. The result for either line shape was a single peak, centered at the weighted mean energy of the doublet, 1253.6 eV. We therefore assume, in assigning energies, that the Mg K α radiation can be approximated by a single line of energy 1253.6 eV.

The substrate was a tungsten crystal oriented within 1° of the (110) plane. It was cleaned by oxygen treatment in the usual manner. Xe and Kr were Linde 99.9999% purity gases used without further purification. As described previously, [10] the crystal could be cooled to 25 K or heated electrically to $T > 2500$ K. Spectra were taken with the crystal at 25 K. An effusion source surrounded by a liquid H₂ cooled cryoshield permitted dosing only the front surface of the crystal. In most Xe and all Kr experiments the cryoshield mask was reduced in length (for reasons not connected with the present experiments) so that only the central portion of the crystal between the potential leads received a gas deposit. Dosing was carried out with the crystal at 25 K. The exposure necessary to complete one monolayer of inert gas had been determined previously [11], and partial layer doses were proportional to the time necessary to complete one monolayer. The coverages could also be monitored by the relative intensity of the XPS and UPS peaks. When Xe was adsorbed on clean W(110) the coverages determined from dosing times and from UPS and XPS integrated peak intensities agreed within 3% of a monolayer. The background pressure of all gases except He during these experiments was less than 2×10^{-10} Torr. During the UPS experiments the background pressure of He was approximately 5×10^{-9} Torr, but its presence had no effect on the results of these experiments.

In some experiments the crystal was precovered with either oxygen or CO. In experiments with CO precoverage, the crystal was dosed in excess of 1 monolayer at ~ 25 K and then heated to 90 K to desorb any physisorbed CO from the crystal. The CO remaining on the crystal after cooling was a saturated layer of virgin-CO. Similarly, in experiments with O precoverage, the cold crystal was covered with the desired amount of oxygen, heated to the desired temperature, and cooled to < 30 K before dosing with inert gas. The necessary doses of oxygen had been previously determined [12]. The oxygen coverage was determined from the dosing time and agreed with the UPS intensity. Isothermal desorption of Xe from virgin-CO covered tungsten and of Kr from clean tungsten was carried out as described previously [11].

Surface cleanliness was monitored periodically by Auger electron spectroscopy. The work function of clean W(110) was also checked by measuring the width of the He(I) photoelectron spectrum. Since the isothermal desorption kinetics of Xe change from zero to first order in the presence of very small amounts of oxygen [11], isothermal desorption of Xe was also carried out periodically and showed the characteristic kinetics for a clean surface.

A curve-fitting routine allowed fitting experimental peaks to Gaussian or Lorentzian shapes, and also allowed peaks to be decomposed into substates, where necessary. The algorithm used was that developed by Marquardt [13] and described in detail by Bevington [14]. A deconvolution procedure was also used occasionally to determine the extent to which instrument resolution affected peak shapes and widths. This consisted of Fourier transforming the experimental spectra by means of a finite transform after smoothing the data by a standard smoothing routine. The Fourier transform was then divided at each point by the Fourier transform of the instrument response function assumed to be Gaussian. For a pass energy of 10 eV, the FWHM of the instrument was taken to be 160 meV, or $\sigma = 68$ meV, with

corresponding values for higher pass energies. The result was then back transformed to yield the deconvoluted spectrum.

3. RESULTS

Ultraviolet photoelectron spectra of Xe as a function of Xe coverage are shown in Figure 1 for $h\nu = 21.2$ eV. Two things are evident: first, there is a splitting of 0.32 ± 0.04 eV for the $5p_{3/2}$ level at all coverages, even at $\theta = 0.04$ ($\theta = 1$ corresponds to 5.5×10^{14} Xe atoms/cm² [15]); furthermore, there is no shift in the peak positions as a function of Xe coverage. The $5p_{3/2}$ levels are located at 5.64 ± 0.06 eV and 5.96 ± 0.03 eV below E_F and the $5p_{3/2}$ level is 7.13 ± 0.02 eV below E_F . Other quantities are in agreement with those previously measured for adsorbed and gas phase Xe. The spin-orbit splitting is 1.33 ± 0.04 eV (1.306 eV, gas phase) and was determined by the difference in energy between the $5p_{3/2}$ level and the average energy of the $5p_{3/2}$ peaks. Spectra with $h\nu = 40.8$ eV had much reduced intensity; the electron binding energies relative to E_F were 7.0 eV for the $5p_{1/2}$ and 5.6 eV for the $5p_{3/2}$ level. The splitting of the $5p_{3/2}$ level could not be resolved because of the reduced signal to noise ratio. The change in work function with Xe coverage, determined from the width of the UV photoelectron spectrum, agreed with the results of Wang and Gomer [15]; after adsorption of 1 monolayer of Xe, $\Delta\phi = -0.35$ eV.

The coverage independence of the $5p_{3/2}$ splitting suggests that it results from Xe-substrate rather than Xe-Xe interactions, unless Xe forms islands of essentially constant density at all coverages. To test this possibility layers were subjected to heat treatments at many Xe coverages. In one set of experiments the Xe layer was annealed at 55 K for one minute after dosing. Since diffusion occurs at that temperature [16] it was felt that the layer would then form or dissolve islands, or otherwise rearrange. In another set of experiments the final coverage was reached from $\theta = 1$ by thermal desorption at 70 K. These

results are shown in Figure 2 as a plot of the ratio of intensities of the $5p_{3/2}$ low binding energy peak to the $5p_{3/2}$ high binding energy peak versus Xe coverage. The splitting of the $5p_{3/2}$ peak is present even at $\theta = 0.04$; it is absent only when $\theta = 0.06$ was reached by thermal desorption at 70 K.

A spectrum for a Xe coverage of 2 monolayers is shown in Figure 3. The peaks corresponding to emission from the second layer are shifted to higher binding energies relative to the first layer peaks, which are unshifted. For the second layer the $5p_{3/2}$ peak is $E_F - 6.40$ eV and the $5p_{1/2}$ peak is at $E_F - 7.66$ eV; the splitting between these two peaks is 1.26 eV, nearly the value of the gas phase spin-orbit splitting. When two layers are present, the intensities of the second layer peaks are almost double the intensities of the first layer peaks although the amounts of Xe in each layer are equal. Splitting of the $5p_{3/2}$ peak in the first layer can still be seen, but any such splitting for the second layer peak would be masked by overlap with emission from the first layer. The energy difference of the $5p_{3/2}$ and $5p_{1/2}$ peaks in the second layer agrees with the gas phase spin-orbit splitting. In the first layer the difference between the $p_{1/2}$ peak and the mean of the two $5p_{3/2}$ components gave the spin-orbit splitting. This suggests that there is no splitting into $5p_{3/2}$ substates in the second layer.

In order to study the effect of oxygen coadsorption on Xe photoemission, the W(110) surface was precovered with known amounts of oxygen and then heated to 90 K. The resulting spectra are shown in Figure 4 for 1 monolayer of Xe adsorbed on varying amounts of oxygen. As the oxygen coverage is increased both 5p peaks move uniformly to lower binding energies. Figure 5a shows the position of the $5p_{1/2}$ binding energy as a function of oxygen coverage (saturation oxygen coverage at 90 K is $O/W = 0.5$). Also shown in Figure 5a are the changes in work function resulting from oxygen adsorption (in the absence of Xe) determined by Wang and Gomer [15] and by Bauer et al. [17]. Data for $\Delta\phi$ in the

presence of oxygen and Xe are available only for maximum oxygen coverage as a function of Xe coverage. Oxygen increases the work function and Xe decreases it, but the effects are not wholly additive. For example, a monolayer of Xe adsorbed on a saturated oxygen layer preheated to 90 K increases the work function by 0.14 eV over the algebraic sum of the oxygen and Xe $\Delta\phi$ values taken separately. Consequently the $\Delta\phi$ values shown are slightly too low by values up to 0.14 eV at maximum oxygen coverage. Despite this fact, the $5p_{1/2}$ peak positions closely follow the change in work functions resulting from oxygen adsorption, as shown in Figure 5a.

The $5p_{1/2}$ peak broadens considerably with increasing oxygen coverage from 0.3 eV to 0.7 eV FWHM (Figure 5b), but the $5p_{3/2}$ component broadens only slightly, the FWHM increasing from 0.63 eV to 0.83 eV; however, the splitting into substates is washed out at oxygen coverages $\theta/W > 0.07$.

Several spectra were taken with submonolayer Xe and submonolayer oxygen coverages. In every case the observed $5p_{1/2}$ binding energy shifts and peak widths were larger than expected on the basis of Figure 5 for the amount of oxygen present. These results are summarized in Table 1.

There is no shift in the Xe peak positions as a function of Xe coverage when Xe is adsorbed on an ordered layer of oxygen, formed by adsorbing at 25 K to $\theta/W = 0.5$ and heating to $T \sim 400$ K, yielding the well-known $p(2 \times 1)$ LEED pattern. The Xe $5p_{3/2}$ peak is at 6.70 ± 0.05 eV below E_F and the $5p_{1/2}$ peak is at 5.34 ± 0.11 eV below E_F . Just as in the case of Xe adsorbed on a disordered oxygen layer the $5p_{3/2}$ peak is broadened only slightly, its splitting removed and the $5p_{1/2}$ peak broadened by a factor of 2. However, the peaks are not shifted upward as much as for Xe adsorbed on a $\theta/W = 0.5$ layer heated to 90 K where the $5p_{1/2}$ peak is at 6.26 eV and the $5p_{3/2}$ peak is at 4.94 eV below E_F .

Figure 6 shows the UPS results for 1 monolayer of Xe adsorbed on 1 monolayer

of virgin CO. Included for comparison is the spectrum for 1 monolayer of Xe adsorbed on clean W(110). The spectrum of Xe/CO/W(110) has approximately twice the intensity found for Xe/W(110), that is, the same intensity as the second layer of Xe in Xe/Xe/W(110). The $5p_{3/2}$ splitting is the same as that on clean W(110), 0.35 ± 0.04 eV, but the 5p peaks are shifted by 1.3 eV to lower binding energies in the presence of a monolayer of virgin CO. The $5p_{1/2}$ peak width is approximately the same for Xe adsorbed on a virgin CO layer (0.40 eV) as for Xe adsorbed on a clean W(110) surface (0.33 eV). Spectra with $h\nu = 40.8$ eV have approximately the same intensity as for Xe/W(110) and only the two main peaks can be resolved. The $5p_{3/2}$ electron binding energy is 4.52 eV and the $5p_{1/2}$ electron binding energy is 5.86 eV, in good agreement with the He(I) results. For virgin CO/W(110) $\Delta\phi = + 0.5$ eV as determined from the width of the He(I) photoelectron spectrum. Xe adsorption on v-CO causes no further changes in ϕ .

Isothermal desorption of Xe adsorbed on a saturated layer of virgin CO was also carried out. Figure 7 shows the rate of Xe desorption as a function of time at 55.3 K. As previously found [11] for single and multiple layers of Xe adsorbed on clean W(110), the desorption is zero order until a large fraction of the desorbing layer has been removed (in this case 85%); from then on desorption obeys first order kinetics. The amount of Xe adsorbed on saturated virgin CO was found to be equal to that in a single layer of Xe adsorbed on either clean, oxygen covered, or Xe covered W(110). Assuming Arrhenius behavior, that is

$$k = \nu \exp(-E_a/RT), \quad (1)$$

activation energies, E_a , and pre-exponential terms, ν , can be found from the variation of the desorption rate, k , with temperature. These results are plotted in Figure 8, and yield for zero order desorption $E_a = 3.0$ Kcal/mole and

$\nu = 9.6 \times 10^{24}$ atoms/cm²-sec, and for first order desorption $E_a = 3.1$ Kcal/mole and $\nu = 2 \times 10^{11}$ /sec. These values are remarkably similar to those found for the desorption of a second Xe layer from Xe/W(110): for the zero order regime, $E_a = 3.3$ Kcal/mole and $\nu = 5 \times 10^{26}$ atoms/cm²-sec, and for the first order regime $E_a = 3.3$ Kcal/mole and $\nu = 6 \times 10^{12}$ /sec [11].

Several experiments were also carried out with Kr. UPS results for one monolayer of Kr on clean W(110), and for 1 monolayer of Kr on an oxygen saturated surface pre-heated to 90 K are shown in Figure 9. When Kr is adsorbed on clean W(110), the $4p_{3/2}$ state is split into two peaks at 7.47 and 7.16 eV below E_F ; the $4p_{1/2}$ peak is at 8.14 eV. The observed spin-orbit splitting taken as the difference between $4p_{1/2}$ and the mean of the 2 $4p_{3/2}$ component energies is 0.8 eV, somewhat larger than the gas phase value 0.66 eV. When Kr is adsorbed on an oxygen precovered surface, the $4p_{1/2}$ and $4p_{3/2}$ peaks are so broadened as to merge, and are also shifted to lower binding energy. A computer fit to the envelope is shown in Figure 9. On this basis the intensity of the $4p_{3/2}$ peak is increased tenfold; and that of the $4p_{1/2}$ peak twofold relative to clean W.

The X-ray photoelectron spectrum of the 3d and 4d levels for 1 monolayer of Xe adsorbed on clean W(110) is shown in Figure 10. The 3d spin-orbit splitting, 12.7 ± 0.1 eV is in good agreement with the gas phase value (12.60 eV) as is the 4d spin-orbit splitting 2.0 ± 0.1 eV (gas phase, 2.0 eV). Figure 11 shows the effect of oxygen preadsorption upon the 3d XPS peak for two different oxygen treatments: in both cases the surface was saturated with oxygen, then heated to either 90 K or 900 K. The shift to lower binding energies is less for Xe/O/W(900 K) than for Xe/O/W(90 K) as is true in UPS. Both Xe 3d peaks are broadened by about 5% on oxygen precovered surfaces. No shift in the 4d or 3d peak positions with Xe coverage could be seen for any of the surfaces studied. The 3d and 4d levels for Xe adsorbed on a layer of virgin CO were also studied by XPS.

Both levels are uniformly shifted by 1.8 eV to lower binding energies, relative to Xe adsorbed on clean W(110); the energies are 681.4 eV and 668.8 eV below E_F for $3d_{1/2}$ and $3d_{3/2}$ respectively, and 61.5 eV and 59.7 eV below E_F for $4d_{1/2}$ and $4d_{3/2}$ respectively.

The positions of the observed Xe and Kr peaks and the corresponding gas phase electron binding energies are summarized in Table 2.

4. DISCUSSION

4.1 $p_{3/2}$ Splitting

Since neutral Xe has a 1S electronic configuration, it is clear that both the existence of $p_{1/2}$ and $p_{3/2}$ states and any further splitting of the $p_{3/2}$ state refer to the final hole states and cannot be initial state effects. The origin of the $5p_{3/2}$ splitting, has been the subject of some controversy. Wacławski and Herbst [18] first observed a broadening of the Xe $5p_{3/2}$ peak on W(110) and correctly attributed it to an unresolved splitting. They ascribed this to a substrate induced crystal field splitting. However, Antoniewicz [19] and Matthew and Devey [20] pointed out that the magnitude of the splitting would require each of the four nearest neighbor substrate atoms to have a charge of $+0.5e$, and showed that a difference in the image interactions of the $m_j = \pm 3/2$ and $m_j = \pm 1/2$ components of the $p_{3/2}$ hole state with the surface was a more plausible explanation. The $J = 3/2$, $m_j = \pm 3/2$ states have only p_x and p_y character, but the $J = 3/2$, $m_j = \pm 1/2$ states have $2/3 p_z$ character (z being the surface normal) and therefore have more hole density closer to the surface. Thus the $m_j = \pm 1/2$ final hole states will interact more strongly and the corresponding photoelectrons will have lower binding energy. Matthew and Devey calculated a Xe $5p_{3/2}$ splitting of approximately 0.3 eV, in good agreement with the present results. Furthermore, the $J = 1/2$, $m_j = \pm 1/2$ states have $1/3 p_z$ character, so that their relaxation energy will lie between that of the $J = 3/2$ final states.

Consequently, the spin-orbit splitting should be unchanged from the gas phase value if it is defined as the difference between the $5p_{3/2}$ peak and a point midway between the two $5p_{3/2}$ peaks. This is, in fact, observed.

The above suggests that Xe-substrate interactions are responsible for the $5p_{3/2}$ splitting. However, Horn et al. [1] reported that the $5p_{3/2}$ splitting was no longer evident at $\theta < 0.7$ for Xe/Pd(100), and Erskine noted that at $\theta < 0.2$ the $5p_{3/2}$ splitting was not observed for Xe/W(100) [2]. Moreover, both groups report angular dispersion of the $5p_{1/2}$ and $5p_{3/2}$ final state of the order of 0.3 eV. They interpret the dispersion and coverage dependence as evidence of direct overlap of neighboring Xe 5p wave functions and 2 dimensional band formation. While relaxation is important in this model, it is assumed to be the same for all final states.

The present results show no coverage dependence of the splitting and thus seem to support the Xe-substrate rather than the Xe-Xe interaction hypothesis, unless there is island formation even at the lowest coverages studied and if the putative Xe-Xe interaction is independent of whether a Xe atom is at the edge or in the interior of an island. This latter assumption seems most improbable. The reasoning behind this assertion is the following: Suppose that even with the substrate at 25 K impinging Xe atoms with a gas temperature of 200 - 300 K have some mobility. Let us assume than an impinging Xe atom can move, on average, 10 Xe diameters a before stopping. This number is almost certainly too large. Islands could then form even with the substrate at 25 K. On average an island could incorporate atoms from an area $(10 a)^2$. Assuming random impact on this area it would contain, $100 a^2 (\theta/a^2)$ Xe atoms, θ being fractional coverage and $\sim 1/a^2$ the monolayer coverage in atoms/cm². Thus the r.m.s. island radius r would be

$$r \sim 10a (\theta/\pi)^{1/2} \quad (1)$$

The ratio of the number of perimeter to interior atoms P/I , is

$$P/I = 2a/r \quad (2)$$

assuming the edge length per atom to be a , or from Eqs. 1 and 2

$$P/I = 0.2 (\pi/\theta)^{1/2} \quad (3)$$

Values obtained in this way are $P/I = 0.5$ for $\theta = 0.5$, $P/I = 0.8$ for $\theta = 0.2$ and $P/I = 1.8$ for $\theta = 0.04$. Thus the number of edge atoms would be a substantial fraction of the total Xe population at $\theta \leq 0.5$ and changes in θ should therefore produce observable changes in the splitting and possibly in other spectral features as well. No such changes were observed. The only case in which the splitting was not observed occurred on heating to 70 K, leaving a final coverage of $\theta = 0.06$. In this case migration to step sites is probable and these can certainly affect the interaction and hence the intensity ratio. All other attempts at annealing or changing the method of attaining the final coverages left the intensity ratio intact, even though these methods would have changed the Xe distribution on the surface if islands occurred. Thus we are forced to the conclusion that Xe-Xe interactions cannot be responsible for the $5p_{3/2}$ splitting. We have no real explanation for the results of Erskine [2] or Horn et al. [1]. However, their published spectra are of such resolution as not to preclude the existence of splitting even at low Xe coverages.

The fact that the Kr $4p_{3/2}$ hole state is also split with approximately the same energy difference as in Xe supports the image interaction model. The latter predicts this effect; on the other hand band effects should be less important for Kr than for Xe since Kr 4p electrons are more tightly bound than Xe 5p electrons.

The adsorbate-substrate interaction responsible for the $p_{3/2}$ splitting has not been discussed so far in any detail. To a first approximation it can be

considered to be the interaction of the p hole with its image in the metal. On this basis the splitting should be larger for Kr than for Xe. However, the classical approximation overestimates the image interaction at distances $\leq 2 \text{ \AA}$ from the surface [21,22] and so the differences between Xe and Kr may become smaller than expected. Direct evidence for the fact that the classical image potential overestimates the interaction is also provided by the relaxation shifts found in the present work, which are discussed in the next section. Gadzuk [21] has also pointed out that the hole in the adatom will be polarized by its image charge in the metal. Since the $m_j = \pm 1/2$ state is closer to the surface, this polarization should relax it more, thereby increasing the $p_{3/2}$ splitting. This effect will be more important for Xe than Kr because Xe^+ has a larger polarizability than Kr^+ . Both the breakdown of the classical image approximation and the inclusion of the hole polarizability will therefore reduce the magnitude of the $p_{3/2}$ splitting of Kr relative to Xe in the classical image approximation.

4.2 PEAK POSITIONS

The binding energy E of a photoelectron relative to the Fermi level of the substrate corresponds to the energy difference of the vertical transition depicted in Figure 12; it will be considered a positive quantity. It can be expressed as

$$E = I - \phi(x) - V^0(x_0) + V^+(x_0) \quad (4)$$

Here I is the ionization energy of the level under consideration for the gaseous atom A away from the surface, and $-V^0(x_0) = H_a$, the atom's heat of adsorption at the surface (H_a is a positive quantity). $\phi(x_0)$ is the effective work function

at x_0 , which may differ from that at $x = \infty$ if the potential of a surface layer has not built up to its full value $\Delta\phi(\infty)$ at x_0 . Thus, if H_a were zero and the ion did not interact at all with the surface, the position of a level would be I volts below the local vacuum level and $E = I - \phi(x_0)$. $V^+(x_0)$ is the energy of interaction of the ion with the substrate, measured from a slightly artificial zero of energy, namely that of the ion at infinite separation from the surface assuming that the work function there is not $\phi(\infty)$ but $\phi(x_0)$. Thus the zero of the $M^- + A^+$ curve is assumed to lie above that of the $M + A$ curve by an energy $I - \phi(x_0)$. Relative to this zero of energy $V^+(x_0)$ is negative for the situation depicted in Figure 12. If $H_a + V^+(x_0)$ varies very little from metal to metal and from plane to plane, peaks should shift quantitatively with the substrate work function as found for Xe by Ertl et al. [4-7]. These authors used the argument just given in slightly different language, to explain these results. They also found a quantitative shift of Xe peaks with oxygen induced work function increases, as also found by us: Figure 5 shows that the shift of Xe peaks to lower binding energies just equals $\Delta\phi$ resulting from various oxygen coverages. On the other hand Xe adsorption also changes ϕ but no change in peak positions with Xe coverage was seen by us for clean or 0 covered W(110) within experimental error. The reason for this is that Xe atoms experience the full substrate work function and the full $\Delta\phi$ caused by oxygen, (i.e. $\phi(x_0) = \phi(\infty)$ for this case), but do not experience the full $\Delta\phi$ of the Xe layer. This is so because at $x_0 = 2.3 \text{ \AA}$, the distance of Xe in the first layer from the surface, the dipole layer potential for O has built up to its full value $\Delta\phi(\infty)$, but that of a Xe layer has built up only to a fraction of $\Delta\phi(\infty)$ at that distance. Figures 13 and 14 show layer potential changes vs. distance at various coverages for Xe and for O on a metal surface, assuming

for oxygen a charge at 0.8 \AA above the surface and for Xe a charge at 2.3 \AA above the surface, the images being at the corresponding distances below the surface. These data were obtained by dipole summations. Xe sees effectively the full $\Delta\phi$ resulting from 0 adsorption, but at $\theta_{\text{Xe}} = 1$ only 25% of $\Delta\phi_{\text{Xe}}$. Since the latter is -0.35 eV on W(110), shifts resulting from Xe adsorption are too small to be seen. On W(111), however, $\Delta\phi_{\text{Xe}} > 1.0 \text{ eV}$ [23] and appreciable shifts should occur, as observed by Yates et al. [8].

There is a difference between the spectra of Xe adsorbed on oxygen heated to 90 K and oxygen heated to $T > 400 \text{ K}$. While the Xe peak positions reflect the full $\Delta\phi(\infty)$ for oxygen heated to 90 K, this is not the case for oxygen layers heated to $T > 400 \text{ K}$. $\Delta\phi(\infty)$ in the latter case is only slightly less, 0.8 eV versus 0.9 eV , but the shift in the 3d and 5p levels is only 0.45 eV . We have no real explanation for this result. It is possible that the surface becomes reconstructed at 900 K and less metallic in the sense that the effective image plane moves in from the surface toward the interior of the metal, because of a lower density of screening electrons, thus decreasing the image potential contribution to V^+ .

So far we have not discussed the absolute positions of levels or equivalently their shifts relative to gas phase values. It is clear from Eq. 4 that these shifts, or decreases in electron binding energy are given, at $x = x_0$ by

$$E - E_{(\text{gas})} \equiv \Delta E = E - [I - \phi(x_0)] = H_a + V^+(x) \quad (5)$$

As already pointed out for adsorption on clean metals or 0 layers and almost certainly for layers of Xe on CO or of Xe on Xe covered surfaces (i.e. for second layers) $\phi(x_0) = \phi(\infty)$. The dominant contribution to V^+ is the image interaction of the hole with the surface. It is given classically by

$$V_{\text{im}} = -e^2/4x = -3.6/x \quad (6)$$

where the second form refers to energy in eV and distance in Å. For "jellium" Eq. 6 has been corrected [22,24] by replacing x by $x - \delta$.

$$V_{im} = e^2/4(x-\delta) \quad (7)$$

This is based on the assumption that the adsorbate touches the positive jellium edge and that the image plane is moved outward from the layer by an electron spillover distance δ (~ 0.8 Å for metals with the electron density of W).

If the contribution to V^+ from effects other than image interaction is nearly equal to the binding in the ground state, i.e., if

$$H_a \approx -(V^+ - V_{im}) \quad (8)$$

the shift ΔE is given by

$$\Delta E \approx V_{im} \quad (9)$$

that is, ΔE is negative, corresponding to a shift upward toward the Fermi level. The difference between H_a and $(V^+ - V_{im})$ can vary with the location of the hole in A^+ . For instance, if A^+ corresponds to the formation of hole in an inner shell, $-(V^+ - V_{im})$ could more nearly equal to H_a than for a hole in the valence shell. This is obviously true for strong adsorption and it is interesting to consider the possibility of such an effect for inert gas adsorption. For Xe on clean W(110), $\phi = 5.3$ eV, the experimental $-\Delta E$ values are 1.01 ± 0.05 eV for $5p_{1/2}$, and the mean of $5p_{3/2}$; 0.9 ± 0.2 eV for $4d$; and 1.15 ± 0.1 eV for $3d$. These values are essentially equal, given the experimental error of the XPS measurements. This equality suggests that differences in $H_a + (V^+ - V_{im})$ are small for different levels. Since H_a for Xe is ~ 0.22 eV (possibly somewhat higher, since only the activation energy was measured and is known to be somewhat smaller than H_a [11]) this is not very surprising. If it is next assumed that $H_a = -(V^+ - V_{im})$, so that Eq. 9 applies, we find that ΔE is

in very bad agreement with the predicted image shift. For Xe $x_0 = 2.3 \text{ \AA}$, $\delta \approx 0.8 \text{ \AA}$, so that Eq. 7 predicts $-\Delta E = 2.4 \text{ eV}$, over twice the value found. Alternatively, if the experimental value, 1 eV , is used with Eq. 7 to find $(x-\delta)$, a value of 3.6 \AA results, which is much too large. Even if $(V^+ - V_{im}) = 0$, addition of $H_a = 0.22 \text{ eV}$ to $-\Delta E = 1 \text{ eV}$ does not bring it up to the value of V_{im} predicted by Eqs. 6 and 7. The most probable cause is the inadequacy of Eq. 7. It seems reasonable to assume for transition metals that the correction should in fact go the other way: The image plane is not at the surface but displaced inward from it by approximately the screening length [25]. Thus the effective charge-image charge separation is $2(x + \delta)$ and

$$V_{im} = -e^2/4(x + \delta) \quad (10)$$

On this basis the calculated value of V_{im} becomes -1.16 eV , in much better agreement with the experimental ΔE values. For Kr, the experimental values of $-\Delta E$ are 1.23 eV for $4p_{1/2}$ and 1.38 eV for $4p_{3/2}$. If $x_0 = 2.1 \text{ \AA}$ and $\delta = 0.8 \text{ \AA}$ are used in Eq. 7, $V_{im} = -2.7 \text{ eV}$ obviously in disagreement with experiment. If Eq. 10 is used $V_{im} = -1.24 \text{ eV}$, again in good agreement with $-\Delta E$. For Kr, H_a is $\sim 0.1 \text{ eV}$, so that it cannot affect ΔE appreciably.

For Xe on Xe/W(110) the effective work function is $5.3 - 0.35 = 4.95 \text{ eV}$, since the contribution -0.35 eV from the first layer is fully in effect at $x = 6.9 \text{ \AA}$, the distance of the center of Xe atoms in the second layer from the surface. On this basis the experimental value $\Delta E = -0.94 + 0.05 \text{ eV}$ is found for $5p$. Application of Eqs. 7 or 10 yields $V_{im} = -0.45$ or -0.6 eV , depending on whether $x + \delta$ or $x - \delta$ is used. Both these values are too low because they ignore the polarization of the first Xe layer by a hole in the second one. If the classical image approximation, Eq. 6 is used, it was shown by D. Bowman [26] that the total energy reduction is given by

$$E_{\text{rel}} = \frac{-e^2}{4s} [x + (1-\alpha^2) \int_0^1 (y^{-a/s} + \alpha)^{-1} dy] \quad (11)$$

where

$$\alpha = \frac{\epsilon - 1}{\epsilon + 1} \quad (12)$$

and ϵ is the dielectric constant of the intermediate layer; a is the thickness of the dielectric layer, and s is the distance of the (point) charge from the outer surface of the dielectric layer. Figure 15 shows graphs of $E_{\text{rel}}/(-e^2/4s)$ vs. $s/(s+a)$ for several values of ϵ . Eq. 11 with $a = 5.0 \text{ \AA}$, $s = 2.5 \text{ \AA}$ and $\epsilon = 2.25$ yields $E_{\text{rel}} = -0.9 \text{ eV}$, in good agreement with the experimental value $\Delta E = -0.9 \text{ eV}$. The omission of $\pm\delta$ at these large distances does not introduce a very serious error either way.

For Xe adsorbed on a layer of virgin CO, the experimental 5p relaxation energy is $1.64 \pm 0.05 \text{ eV}$, and the 3d and 4d relaxation energies are $1.7 \pm 0.2 \text{ eV}$. These values are again much higher than pure image interactions. If the CO polarization is taken into account by Eq. 11 using $s = 6 \text{ \AA}$ and $a = 3 \text{ \AA}$, a value of $\epsilon = 7$ would be required to give the observed ΔE . This ϵ is unphysically high for condensed CO. The large relaxation energy is particularly surprising since the peaks are not appreciably broadened and the splitting of the $5p_{3/2}$ peak is not affected. As noted previously, thermal desorption measurements indicate that Xe desorbs from a virgin layer with $E_a = 3.0 \text{ Kcal/mole}$, which is almost identical to that found for second layer Xe desorption. Thus there are no obvious initial state effects involved. It is possible that virgin CO on W(110) is more polarizable than free CO, because back bonding partially fills the CO 2π orbitals. High polarizability could also account for the lifting of the degeneracy of the $m_j = \pm 1/2$ and $m_j = \pm 3/2$ hole states just as in the interaction of Xe with a clean surface.

It is interesting to compare the ΔE values obtained in the present work with other results, where overlap exists. Kaundl et al. [9] find, for Xe on Pd(100) a shift of -1.71 eV for Xe 5p; however, these authors assumed the full $\Delta\phi_{\text{Xe}} = -0.65$

eV to be effective. If this is subtracted, a value of $\Delta E = -1.1$ eV results, in good agreement with the present work. A value of -1.13 eV was found, independent of θ_{Xe} , by Horn et al. [1] for Xe 5p on Pd(100). For Xe 4p Kaindl et al. [9] find $\Delta E = -1.5$ eV (correcting their results by excluding $\Delta\phi_{\text{Xe}}$). This value is significantly higher than that found by us for Xe 4p or 3d. We have no explanation for this discrepancy. Kaindl et al. [9] also examined shifts for Xe in higher layers and find, as we do, that polarization effects are important.

4.3 PHOTOEMISSION LINE SHAPES

There are many contributions to the measured photoemission line shapes. Among the most important are instrumental broadening, many electron effects, final state lifetimes, and Franck-Condon overlaps. Citrin, Wertheim and Baer [27] have considered the effects of instrumental broadening on measured line shapes and have deconvoluted the instrumental response from their measured spectra. We were able to remove instrumental broadening with the deconvolution procedure already described. With the exception of the Xe 5p peaks on clean W(110), the deconvolution narrowed the peaks only slightly, by $\sim 5\%$. The Xe 5p peaks on clean W(110) were narrowed by $\sim 20\%$ and the $5p_{3/2}$ splitting was better resolved. However, small oscillations were introduced into the spectrum (Fig. 16) because of the finite cutoffs of the Fourier transforms. In general, the instrument response did not effect our results significantly.

Since the minimum of the $W^- + \text{Xe}^+$ potential curve lies closer to the surface than that of the $W + \text{Xe}$ curve, Franck-Condon transitions will couple the initial state wave function with many final vibrational states. As a result, the Franck-Condon envelope will be broadened and roughly Gaussian because of the Gaussian probability amplitude of the ground vibrational state. There will be two components to this envelope, the zero point (zero temperature) width and a tempera-

ture dependent part reflecting the occupation of higher initial vibrational states at finite temperatures. Recently, Gadzuk et al. [28] have shown that the temperature dependence contributes approximately 30% to the overall width of the $5p_{1/2}$ emission for Xe adsorbed on Cu(110) at 30 K. Even when all these factors were removed FWHM of Xe 5p and Kr 4p peaks on clean W(110) are 0.2 - 0.3 eV. If this residual broadening is interpreted purely in terms of hole lifetime

$$\tau = \hbar / \text{FWHM} \quad (13)$$

values of $\tau \approx 3 \times 10^{-15}$ sec result. Electron stimulated desorption studies of Xe, and particularly Kr on W(110) [29] indicate, however, that $\tau \sim 10^{-14}$ sec, which corresponds to FWHM = 0.05 eV. If these conclusions are correct, other factors, for instance, the finite time required to "turn on" the image interaction must be responsible for the observed widths.

Doniach, and Sunjic [30] and Gadzuk [31] have considered many-electron effects in photoemission. They have shown that suddenly switching on a hole results in the creation of many low energy electron-hole pairs. The observed line shape will vary from a Lorentzian at very slow (adiabatic) switching times to a line shape strongly skewed to higher binding energies at fast (sudden) switching times. This has, in fact, been observed experimentally by Citrin et al. [27]. The $5p_{1/2}$ peak for Xe/W(110) has an asymmetry index of 1.05, defined as the ratio of the high binding energy half-width to the low binding energy half-width; the half-width is defined as the energy difference between the peak and at half the maximum intensity. As expected, this asymmetry is small because of the low energy of the final electron and the correspondingly long switching time. However, this does not exclude broadening resulting from the finite time required for turning on the charge distribution.

Figures 4 and 9 show that the Xe 5p and Kr 4p peak shapes are affected by oxygen. O removes the splitting of the $5p_{3/2}$ peak but does broaden this peak significantly. On the other hand, the $5p_{1/2}$ peak is substantially broadened. For Kr adsorbed on oxygen layers broadening was so much that separate $4p_{1/2}$ and $4p_{3/2}$ peaks could no longer be resolved. However, a curve fitting routine allowed approximate decomposition into $4p_{1/2}$ and $4p_{3/2}$ peaks (Fig. 17). Figures 18 and 19 show the increase in FWHM for Xe and Kr peaks as a function of oxygen UPS intensity at the energies of the Xe and Kr peaks. There is a strong correlation between UPS intensity resulting from O adsorption, i.e. O 2p density of states, and broadening. This suggests that the latter arises from reduced hole lifetimes because of resonance tunneling from O 2p states. On clean W the predominant mechanism of neutralization is interatomic Auger decay via the W d- band, which terminates ~ 5 eV below E_F . While there is a broad s-band its DOS and probably its overlap with Kr and Xe 5 or 4p orbitals is weak, so that resonance tunneling will not contribute appreciably on clean W. Since interatomic Auger decay should be much slower than resonance tunneling when there is comparable overlap, it seems clear that the presence of O 2p DOS can greatly reduce hole lifetimes via resonance tunneling. The fact that different peaks are broadened differently, depending on the O 2p DOS at the peak energies also indicates that the broadenings observed are not the result of anisotropies in the electric field seen by Xe or Kr atoms in different positions on the surface. The reduced hole lifetimes postulated here also serve to explain the inhibition of Kr electron stimulated desorption, seen by Zhang and Gomer [29].

For Xe on CO/W(110) only very slight broadening of the 5p peaks was observed. CO does not have significant 4σ density of states at the energies of these peaks. While there is some $5\sigma - 1\pi$ density of states at these energies, the spatial overlap of these orbitals with Xe must be small for geometric reasons. Thus, the hole

lifetimes for Xe adsorbed on virgin CO could be approximately the same as on a clean tungsten surface.

The strong coupling of the final state ion to the oxygen electronic density of states has another effect. The Xe 5p peaks and Kr 4p_{1/2} peak are increased slightly in intensity, while the Kr 4p_{3/2} peak intensity increases dramatically. Since the final density of states is increased as a result of the coupling to the oxygen density of states is increased the transition moment, proportional to the final density of states, is also increased.

Table 1 and Figure 5 indicate that the coadsorption of submonolayer coverages of Xe and submonolayer (i.e. $\theta_0 < 0.5$) amounts of O lead to more broadening of Xe 5p_{1/2} peaks and also to greater shifts than would be expected purely on the basis of $\Delta\phi_0$ at the respective coverages. This suggests that Xe atoms seek out O atoms, i.e. migrate to the vicinity of O. An adequate mobility for impinging Xe atoms is not surprising, since they need not migrate more than 1-3 Xe diameters to reach O even at $\theta < 0.1$. Previous work by us indicates that the presence of O increases the binding energy of Xe [11] in agreement with this observation. The occurrence of larger level shifts at intermediate Xe coverage than at full Xe coverage (for constant θ_0) is explained by the fact that Xe atoms no longer can seek out O atoms at $\theta_{\text{Xe}} = 1$.

4.4 PHOTOEMISSION INTENSITIES

The He(I) UPS intensity of Xe adsorbed on either a monolayer of Xe or a monolayer of virgin-CO is increased by a factor of 2 over that of Xe adsorbed on clean W(110). However, the He(II), $h\nu = 40.8$ eV, photoelectron spectrum shows little, if any, increase for Xe adsorbed on virgin CO. It is unlikely that different surfaces have a large effect on the transition moment for photoemission of electrons from Xe

for a given photon energy. Since the principal difference between the He(I) and He(II) spectra is the energy of the emitted electrons, the differences in relative intensity just cited must result from varying abilities of the underlying atoms to scatter photoelectrons of different energy. Furthermore, the elastic differential and integrated electron scattering cross sections of gas phase CO show a strong energy dependence in the range from 1 to 100 eV. The integrated elastic scattering cross section drops from $11 \times 10^{-16} \text{ cm}^2$ at 15 eV, approximately the Xe $5p_{1/2}$ He(I) kinetic energy, to $6.6 \times 10^{-16} \text{ cm}^2$ at 30 eV, roughly the Xe $5p_{1/2}$ He(II) kinetic energy [32]. The Xe differential elastic cross section is roughly twice that of CO at most electron energies and angles [33], but the Xe coverage at saturation is about half that of saturation virgin CO coverage ($\theta_{\text{CO}} = 11.4 \times 10^{14} \text{ molecules/cm}^2$; $\theta_{\text{Xe}} = 5.5 \times 10^{14} \text{ atoms/cm}^2$). Thus, the intermediate Xe and virgin CO layers appear to be equally good elastic electron scatterers but better than clean W(110) at He(I) Xe 5p photoelectron kinetic energies. At Xe 5p He(II) kinetic energies, however, virgin CO and clean W(110) are comparable.

ACKNOWLEDGEMENT

This work was supported in part by ONR Contract N00014-77-C-0018. We have also benefitted from support by the Materials Research Laboratory of the National Science Foundation at the University of Chicago.

REFERENCES

- [1] K. Horn, M. Scheffler and A. M. Bradshaw, Phys. Rev. Lett. 41 (1978) 822.
- [2] J. L. Erskine, Phys. Rev. B24 (1981) 2236.
- [3] J. Küppers, F. Nitschke, K. Wandelt and G. Ertl, Surface Sci. 88 (1979) 1.
- [4] K. Küppers, K. Wandelt and G. Ertl, Phys. Rev. Lett. 43 (1979) 928.
- [5] K. Küppers, H. Michel, F. Nitschke, K. Wandelt and G. Ertl, Surface Sci. 89 (1979) 361.
- [6] J. Hulse, J. Küppers, K. Wandelt and G. Ertl, Appl. Surf. Sci. 6 (1980) 453.
- [7] K. Wandelt, J. Hulse and J. Küppers, Surface Sci. 104 (1981) 212.
- [8] J. T. Yates and N. E. Erickson, Surface Sci. 44 (1974) 489.
- [9] G. Kaindl, T.-C. Chiang, D. E. Eastman and F. J. Himpsel, Phys. Rev. Lett. 45 (1980) 1808.
- [10] Ch. Steinbrüchel and R. Gomer, Surface Sci. 67 (1977) 21.
- [11] R. Opila and R. Gomer, Surface Sci. 112 (1981) 1.
- [12] R. Opila and R. Gomer, Surface Sci. 105 (1981) 41.
- [13] Donald W. Marquardt, J. Soc. Ind. Appl. Math. 11 (1963) 431.
- [14] Phillip R. Bevington, Data Reduction and Error Analysis for the Physical Sciences (McGraw-Hill, Inc., New York, 1969).
- [15] C. Wang and R. Gomer, Surface Sci. 84 (1979) 329.
- [16] J.-R. Chen and R. Gomer, Surface Sci. 94 (1980) 456.
- [17] T. Engel, H. Niehus and E. Bauer, Surface Sci. 52 (1975) 237.
- [18] B. J. Wacławski and J. F. Herbst, Phys. Rev. Lett. 35 (1975) 1594.
- [19] P. R. Antoniewicz, Phys. Rev. Lett. 38 (1977) 374.
- [20] J.A.D. Matthew and M. G. Devey, J. Phys. C9 (1976) L413.
- [21] J. W. Gadzuk, Phys. Rev. B14 (1976) 2267.
- [22] J. A. Appelbaum and D. R. Hamann, Phys. Rev. B6 (1972) 1122.
- [23] T. Engel and R. Gomer, J. Chem. Phys. 52 (1970) 5572.
- [24] N. D. Lang and W. Kohn, Phys. Rev. B7 (1973) 3541.

- [25] L. W. Swanson and R. Gomer, J. Chem. Phys. 39 (1963) 2827; D. M. News, J. Chem. Phys. 50, (1969), 4572.
- [26] D. Bowman, private communication.
- [27] P. H. Citrin, G. K. Wertheim and Y. Baer, Phys. Rev. B16 (1977) 4256.
- [28] J. W. Gadzuk, S. Holloway, C. Mariani and K. Horn, Phys. Rev. Lett. 48 (1982) 1288.
- [29] Q.-J. Zhang and R. Gomer Surface Sci. 109 (1981) 567; Q.-J. Zhang, R. Gomer and D. Bowman, to be published.
- [30] S. Doniach and M. Šunjić, J. Phys. C3 (1970) 285.
- [31] J. W. Gadzuk and M. Šunjić, Phys. Rev. B12 (1975) 524.
- [32] H. Tanaka, S. K. Srivastava and A. Chutjian, J. Chem. Phys. 69 (1978) 5329.
- [33] J. F. Williams and A. Crowe, J. Phys. B8 (1975) 2233.

TABLE 1
ELECTRON BINDING ENERGIES AND FWHM OF XE $5p_{1/2}$ PEAK FOR
SUBMONOLAYER XE ADSORBED ON SUBMONOLAYER OXYGEN

Xe coverage (monolayers)	O coverage (O/W)	$\Delta\phi_0^a$ (eV)	$5p_{1/2}$ binding energy (eV)	$5p_{1/2}$ FWHM (eV)
1	0.00	0.00	7.13	0.33
0.34	0.09	0.05	7.05	0.68
0.17	0.20	0.10	7.00	0.58
0.17	0.09	0.05	7.09	0.78
1	0.5	0.90	6.26	0.73

TABLE 2
XE AND KR UPS AND XPS BINDING ENERGIES

		Clean W(110) ^a	O/W = 0.5 (90 K) ^a	O/W = 0.5 (900 K) ^a	v-CO/W ^a	Gas Phase ^b
Xe	5p _{3/2}	5.64 ± 0.06	4.93 ± 0.02	5.34 ± 0.11	4.30 ± 0.05	12.130
		5.96 ± 0.03			4.67 ± 0.02	
	5p _{1/2}	7.13 ± 0.02	6.36 ± 0.02	6.70 ± 0.05	5.87 ± 0.02	13.436
	4d _{5/2}	61.3 ± 0.1	—	—	59.7 ± 0.2	67.5
	4d _{3/2}	63.3 ± 0.1	—	—	61.5 ± 0.2	69.5
	3d _{5/2}	670.0 ± 0.1	669.3 ± 0.1	669.6 ± 0.1	668.8 ± 0.1	679.4
Kr	3d _{3/2}	682.7 ± 0.1	682.0 ± 0.1	682.3 ± 0.1	681.4 ± 0.1	689.0
	4p _{3/2}	7.16 7.47	6.75	—	—	14.000
	4p _{1/2}	8.14	7.78	—	—	14.665

All energies reported in eV (a) relative to E_F, (b) relative to vacuum level.

TABLE 3

XE AND KR RELAXATION ENERGIES WHEN ADSORBED ON CLEAN W(110)
AND PEAK SHIFTS UPON COADSORPTION

Peak	Shift relative to clean W(110)			
	(clean W(110))	O/W(110) (90 K)	O/W(110) (900 K)	v-CO/W(110)
Xe	5p _{3/2}	1.03 ^b	0.87 ^b	0.46 ^b
	5p _{1/2}	1.01	0.87	0.43
	4d _{5/2}	0.9	—	—
	4d _{3/2}	0.9	—	—
	3d _{5/2}	1.1	0.7	0.4
	3d _{3/2}	1.0	0.7	0.4
Kr	4p _{3/2}	1.39	0.57	—
	4p _{1/2}	1.23	0.36	—

^a All energies in eV.

^b Xe 5p_{3/2} values on clean and CO covered W(110) are taken as the average of the two components.

FIGURE CAPTIONS

- 1) He(I) photoelectron spectra as a function of Xe coverage on W(110). Curve for $\theta=0.04$ is the sum of four spectra. Pass energy 10 volts. Energies are relative to E_F .
- 2) Ratio of the intensity I_1 , of the low binding energy component to I_2 of the high binding energy component of $5p_{3/2}$ as a function of Xe coverage for different heat treatments. (O) crystal dosed at 30 K; (Δ) annealed at 55 K; (\square) final coverage reached by thermal desorption at 70 K.
- 3) He(I) photoelectron spectrum of 2 monolayers of Xe adsorbed on W(110). Pass energy 15 volts. Energies are relative to E_F .
- 4) He(I) photoelectron spectra of Xe on oxygen precovered surfaces. Varying amounts of oxygen were adsorbed on a cold crystal and heated for 1 minute at 90 K before adsorption of 1 monolayer of Xe. Pass energy is 15 volts. Energies are relative to E_F .
- 5) (a) Xe $5p_{1/2}$ binding energy relative to E_F as function of oxygen coverage (\bullet). Also shown are the results of Wang and Gomer [15], (Δ) and Engel et al. [17], (\square) for the oxygen induced work function change on W(110), $\Delta\phi_0$.
(b) Xe $5p_{1/2}$ peak full width at half maximum (FWHM) as function of oxygen coverage, O/W.
- 6) He(I) photoelectron spectrum of 1 monolayer of Xe on a saturated virgin-CO layer. Included for comparison is a He(I) photoelectron spectrum of 1 monolayer Xe adsorbed on clean W(110). Pass energy is 10 volts. Energies are relative to E_F .
- 7) Mass spectrometer signal versus time for isothermal desorption of Xe in the first layer for a W(110) surface saturated with CO and heated to 90 K, before Xe adsorption.
- 8) Semilogarithmic plots of k_1 , the zero order rate constant and k_1 , the first order rate constant vs. $1/T$ for Xe adsorbed on virgin CO on W(110).

- 9) He(I) photoelectron spectra of Kr adsorbed on clean and oxygen covered W(110) surfaces. Pass energy is 10 volts. Energies are relative to E_F . Photon intensities are equal for both spectra.
- 10) Mg K α photoelectron spectrum of 3d and 4d emission of Xe adsorbed clean W(110). Pass energy is 50 volts. Energies are relative to E_F .
- 11) Mg K α photoelectron spectrum of the Xe 3d $_{3/2}$ peak adsorbed on clean W(110), W(110) covered with oxygen and heated to 90 K before Xe adsorption, and W(110) covered with oxygen and heated to 900 K before Xe adsorption. Energies are relative to E_F .
- 12) Schematic diagram illustrating the change in electron binding energy E with adsorption, relative to the free atom. In all cases these energies are relative to E_F . The potential curve representing interaction of a neutral atom A with the metal M is marked M+A, that representing an ion and the metal (with the electron from A assumed to be in M) is marked $M^- + A^+$. I , ionization potential of A; $\phi(\infty) = -E_F$, work function of metal. $\phi(x_0)$ is the effective work function at the equilibrium distance x_0 of A. H_a , enthalpy of adsorption of A. $V^+(x)$, the potential energy of the ion is measured from a reference point $I - \phi(x_0)$ above the zero of the M+A curve. This corresponds to assuming that the work function at large distances is $\phi(x_0)$ rather than $\phi(\infty)$.
- 13) Dipole layer potential $V(z)$ resulting from O adsorption as function of distance from a W surface, for various positions relative to the 0 p 2 x 1 structure. The p 2 x 1 unit cell is indicated in the inset, with the circles corresponding to O atom positions. The ordinate is normalized in units of the full work function change, $\Delta\phi_0$ resulting from O adsorption, the abscissa is given in units of the tungsten unit cell length, $a_W = 3.16 \text{ \AA}$. The distance of the center of a Xe atom from the (assumed flat) surface is indicated by $r_{Xe} = 2.3 \text{ \AA}$. The oxygen dipole was assumed to consist of a point charge at $a_W/4$ above the surface, with a corresponding image at $a_W/4$ below the surface.

- 14) Dipole layer potential $V(z)$ over an (empty) Xe site resulting from Xe adsorption, as function of distance z from the surface, for various fractional monolayer coverages, θ . The ordinate is normalized in terms of $\Delta\phi_{\text{Xe}}$, the abscissa in terms of Xe radius, $r_{\text{Xe}} = 2.3 \text{ \AA}$. $\theta = 1$ corresponds to $6.6 \times 10^{14} \text{ Xe atoms/cm}^2$.
- 15) Total relaxation energy E_{rel} (image plus polarization) of a charge in front of a conducting surface covered by a dielectric slab, as function of $s/(a+s)$. Here s is the distance of the charge from the outer edge of the dielectric slab, and a the thickness of the slab. The ordinate is given in units of $-e^2/4s$, the classical image potential for infinite dielectric constant. The numbers on the curves are the dielectric constants of the slab.
- 16) Deconvolution of instrument response for a He(I) spectrum of the Xe 5p peaks on clean W(110). The points are the actual spectrum, the line the computer generated spectrum with instrument response removed. The oscillations result from the finite cutoffs of the peaks when carrying out the required Fourier transforms. The instrument response function was assumed to be Gaussian with a FWHM = 240 meV, corresponding to the pass energy of 15 eV used in the analyzer.
- 17) Computer fit to the Kr/O/W(110) spectrum of Figure 9, showing decomposition into $4p_{3/2}$ and $4p_{1/2}$ peaks. Relative intensities based on this fit are $4p_{3/2}$ 10 times intensity on clean W, $4p_{1/2}$ 2 times intensity on clean W(110).
- 18) Broadening of Kr and Xe peaks relative to values on clean W(110) for adsorption on O/W(110) = 0.5 as a function of oxygen UPS intensity at the energies of the various peaks. Oxygen layer prepared as for Figure 4.
- 19) Oxygen induced photoelectron intensity (right ordinate) and increases in oxygen induced FWHM of Xe and Kr peaks (left ordinate) vs. energy (relative to E_F). Also shown are the positions of the peaks relative to E_F on oxygen covered W(110). O/W = 0.5, layer prepared as for Figure 4.

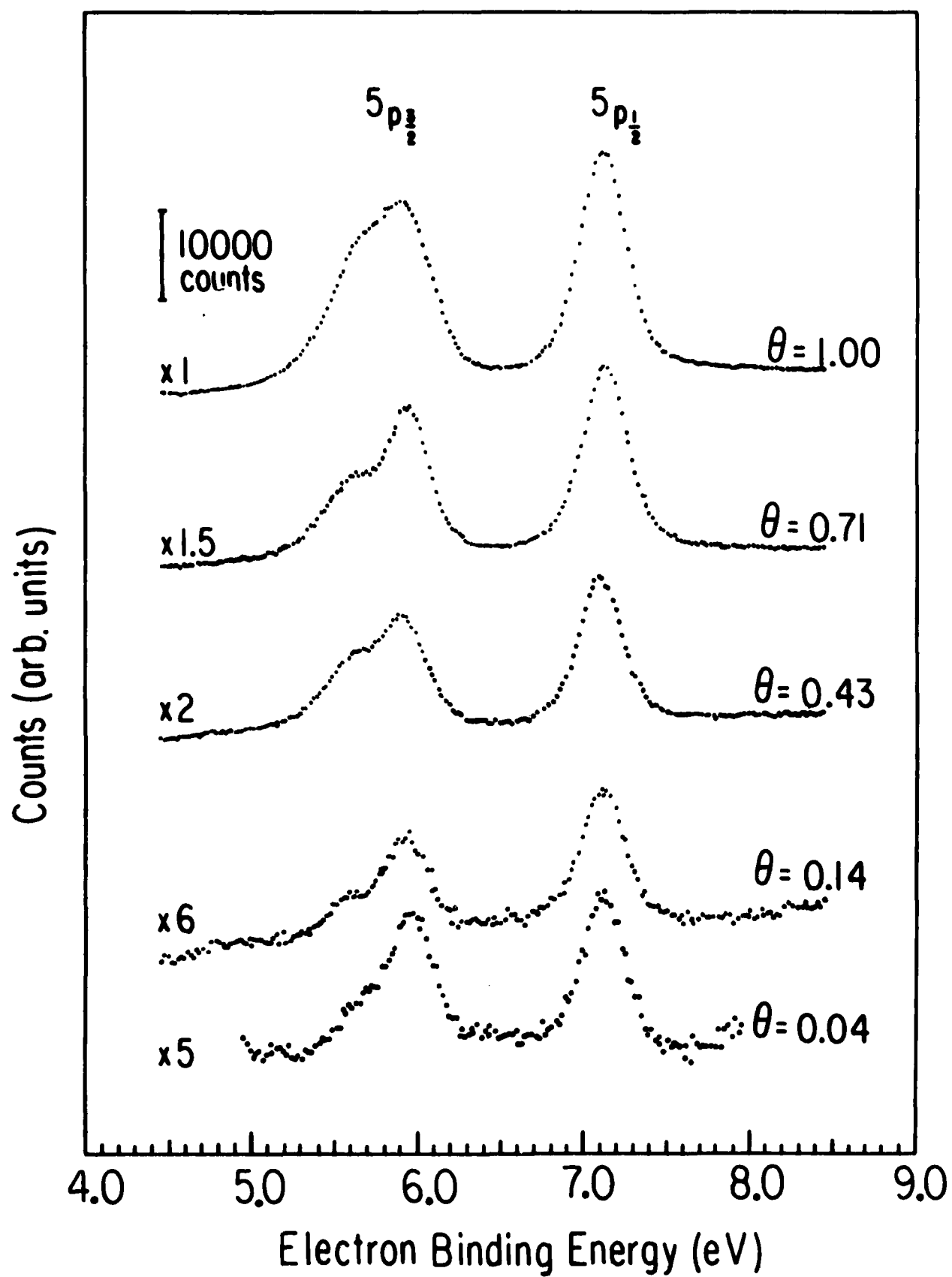


Fig. 1

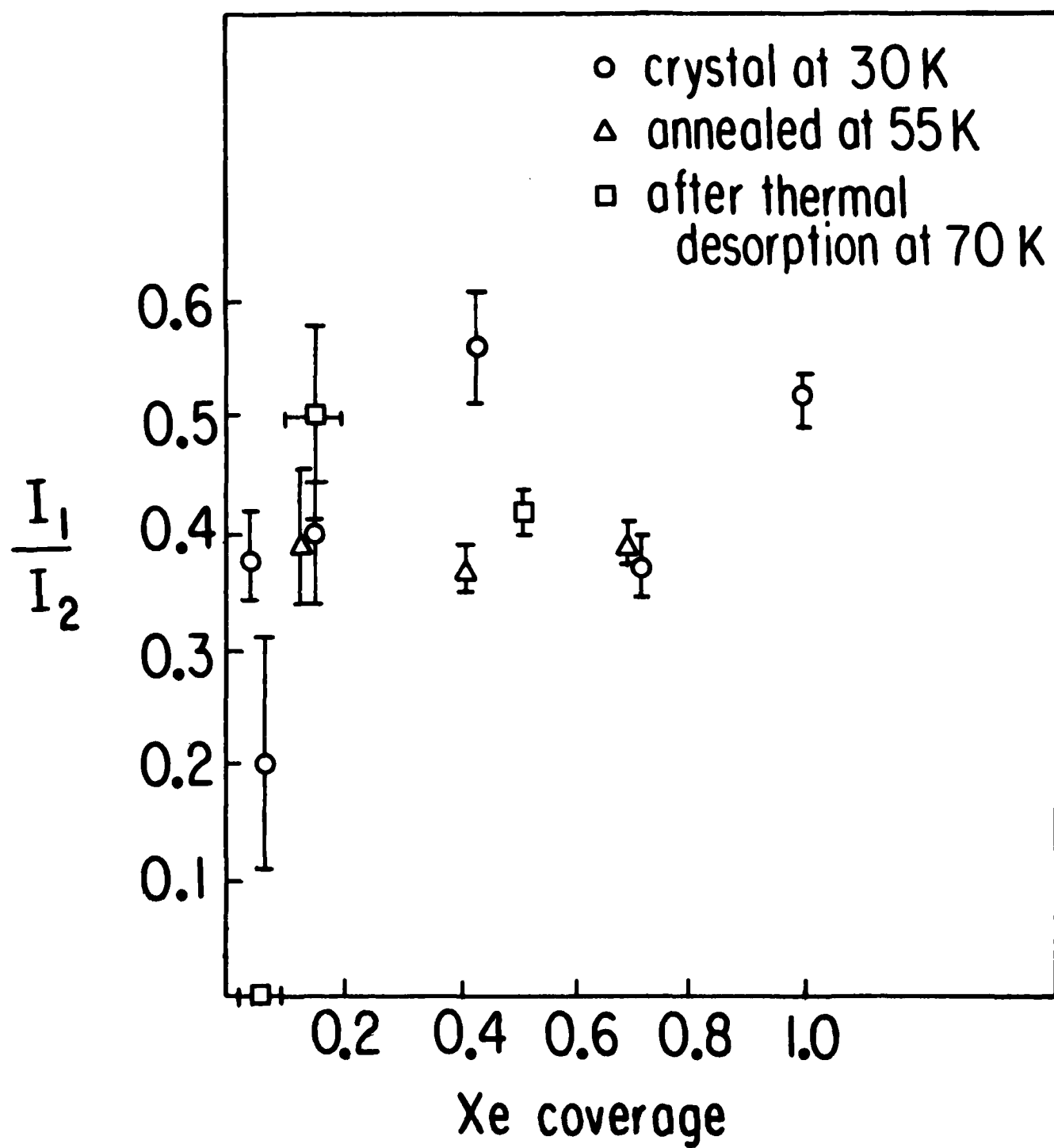


Fig. 2

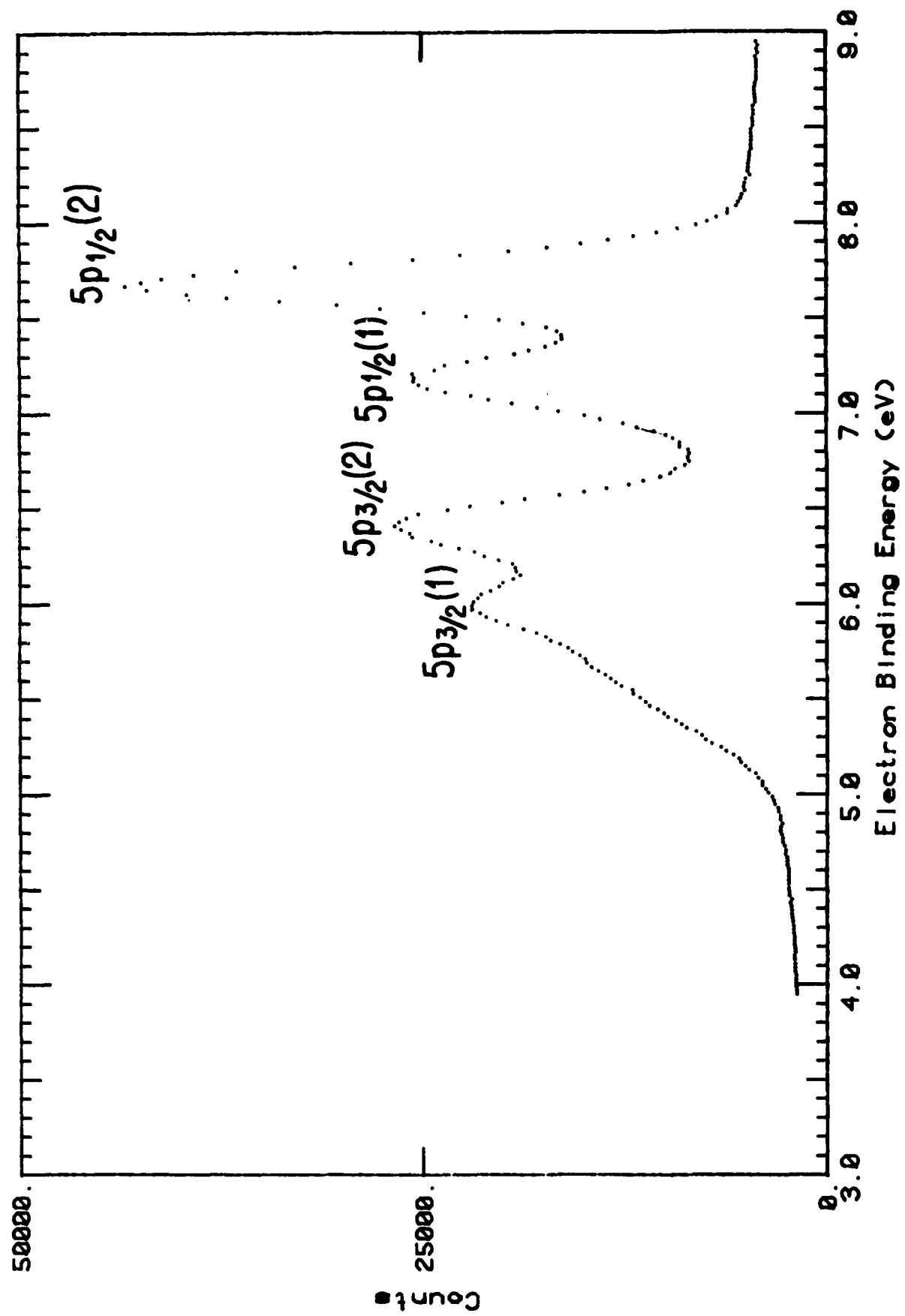


Fig.3

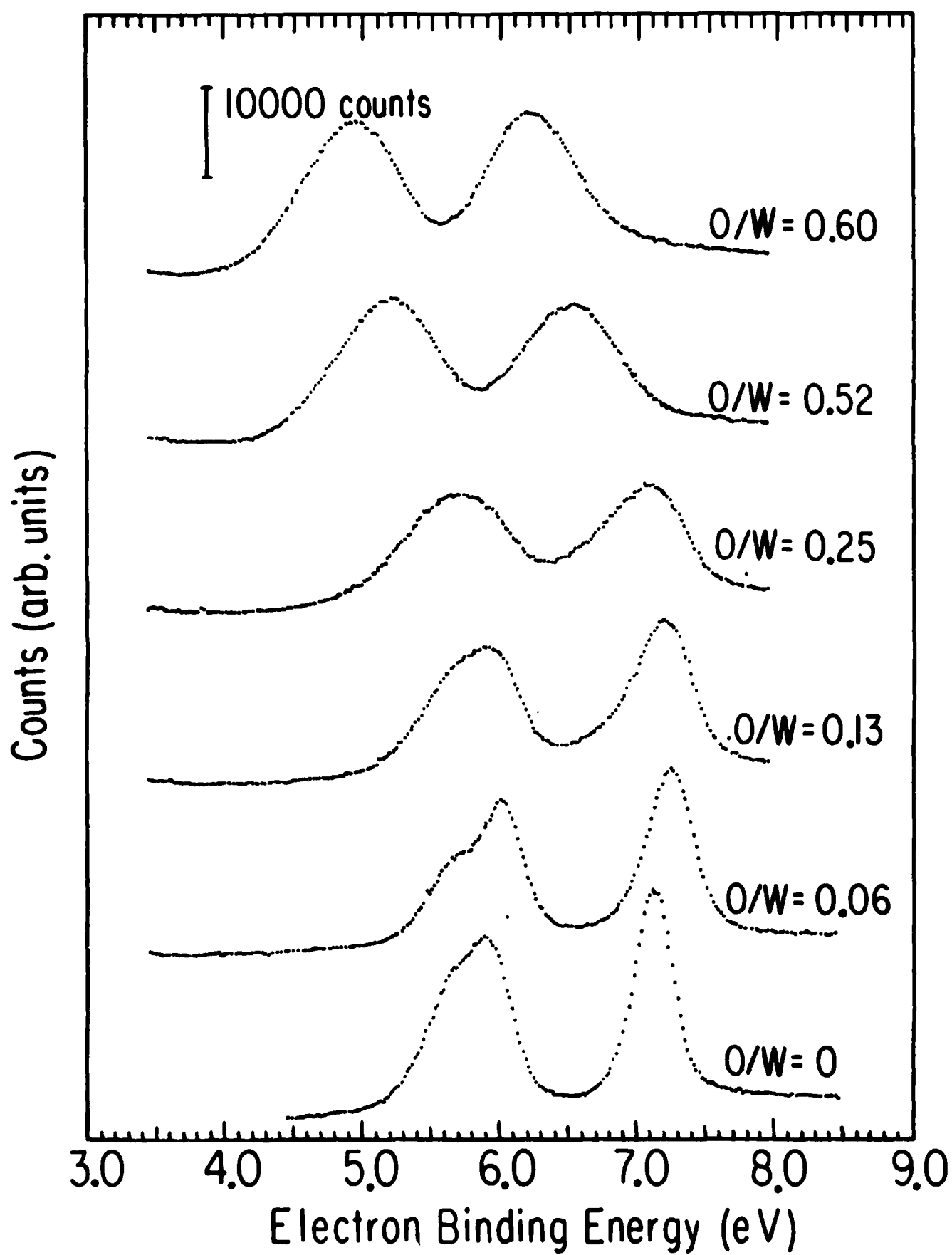


Fig.4

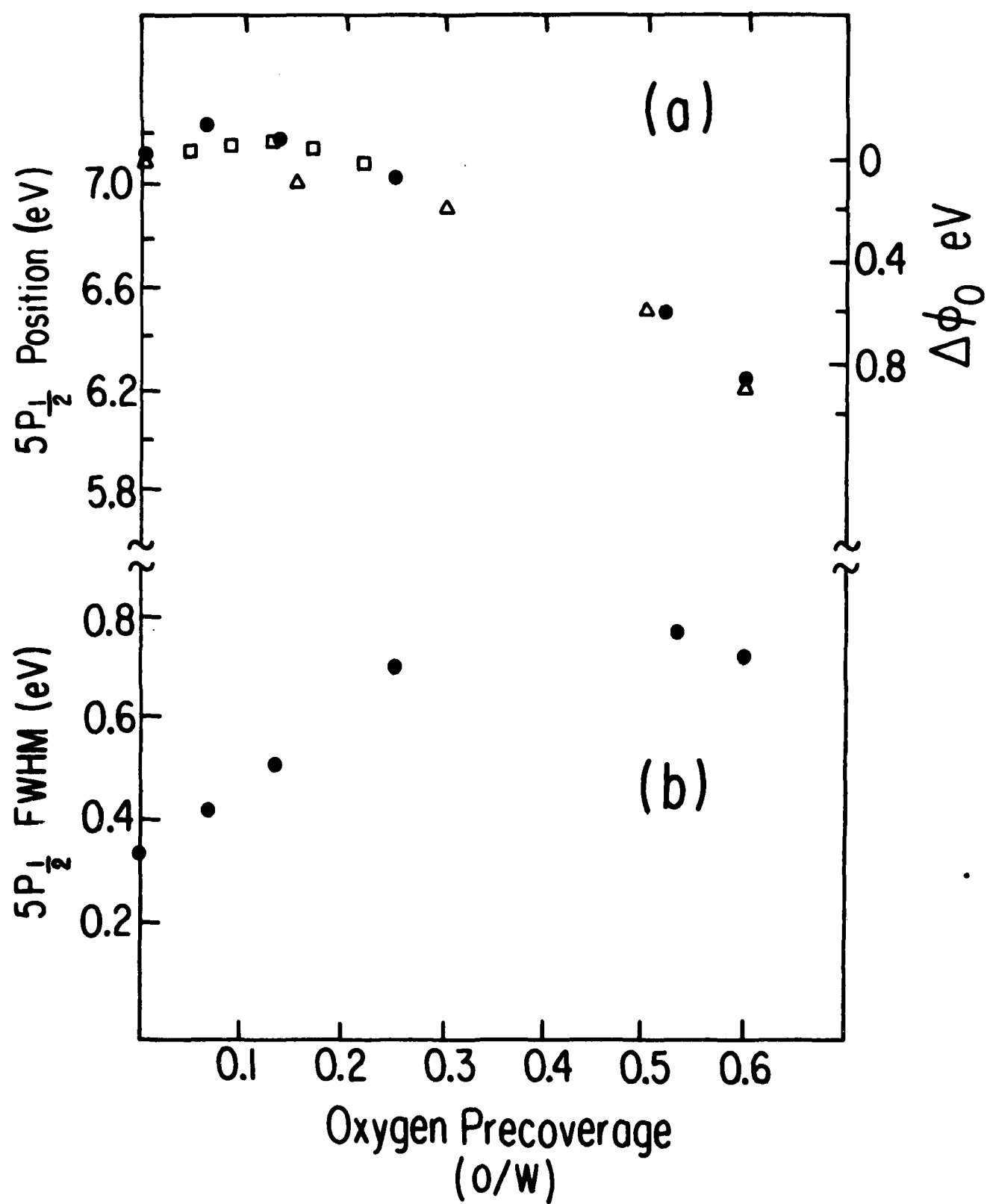


Fig.5

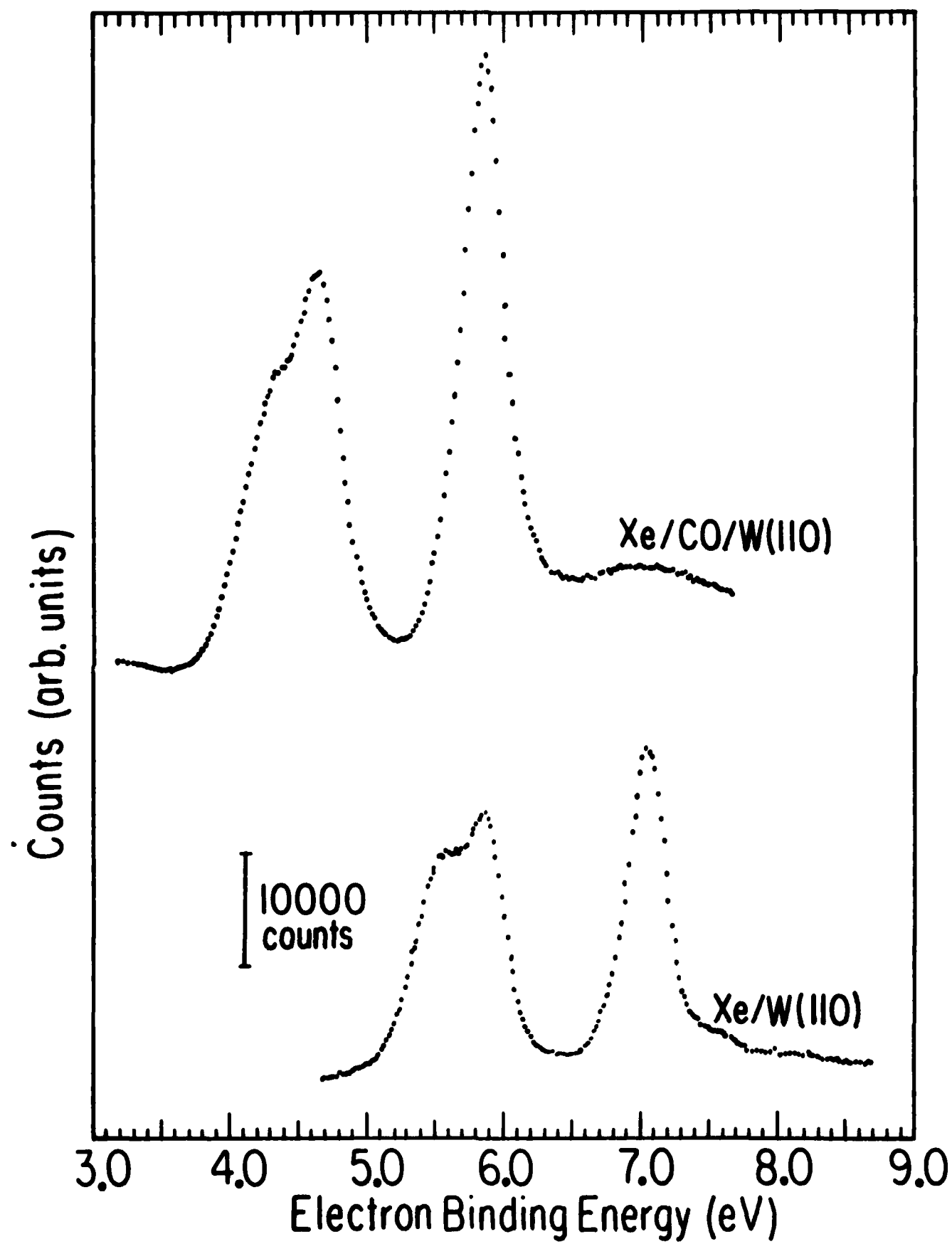


Fig.6

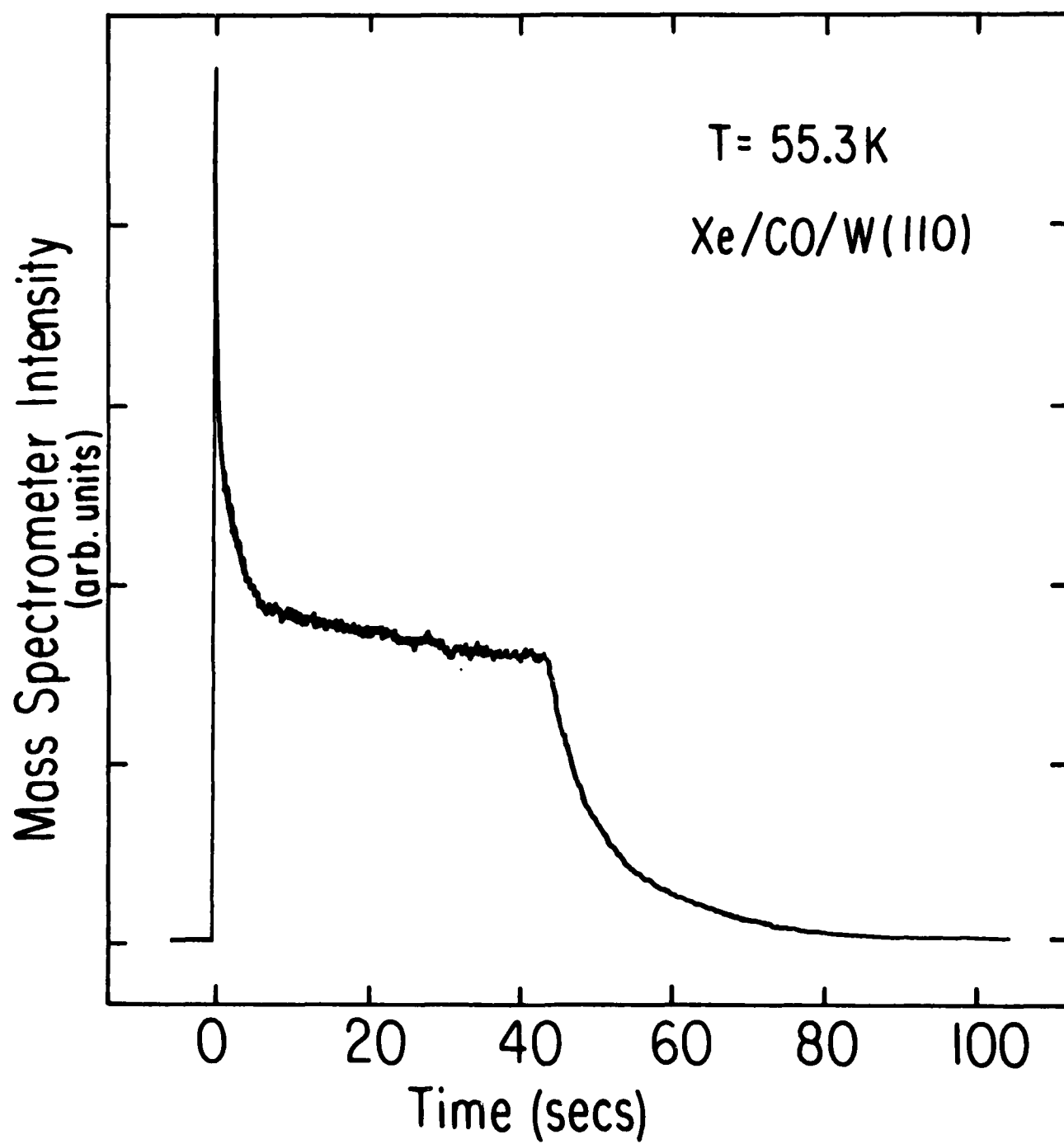


Fig.7

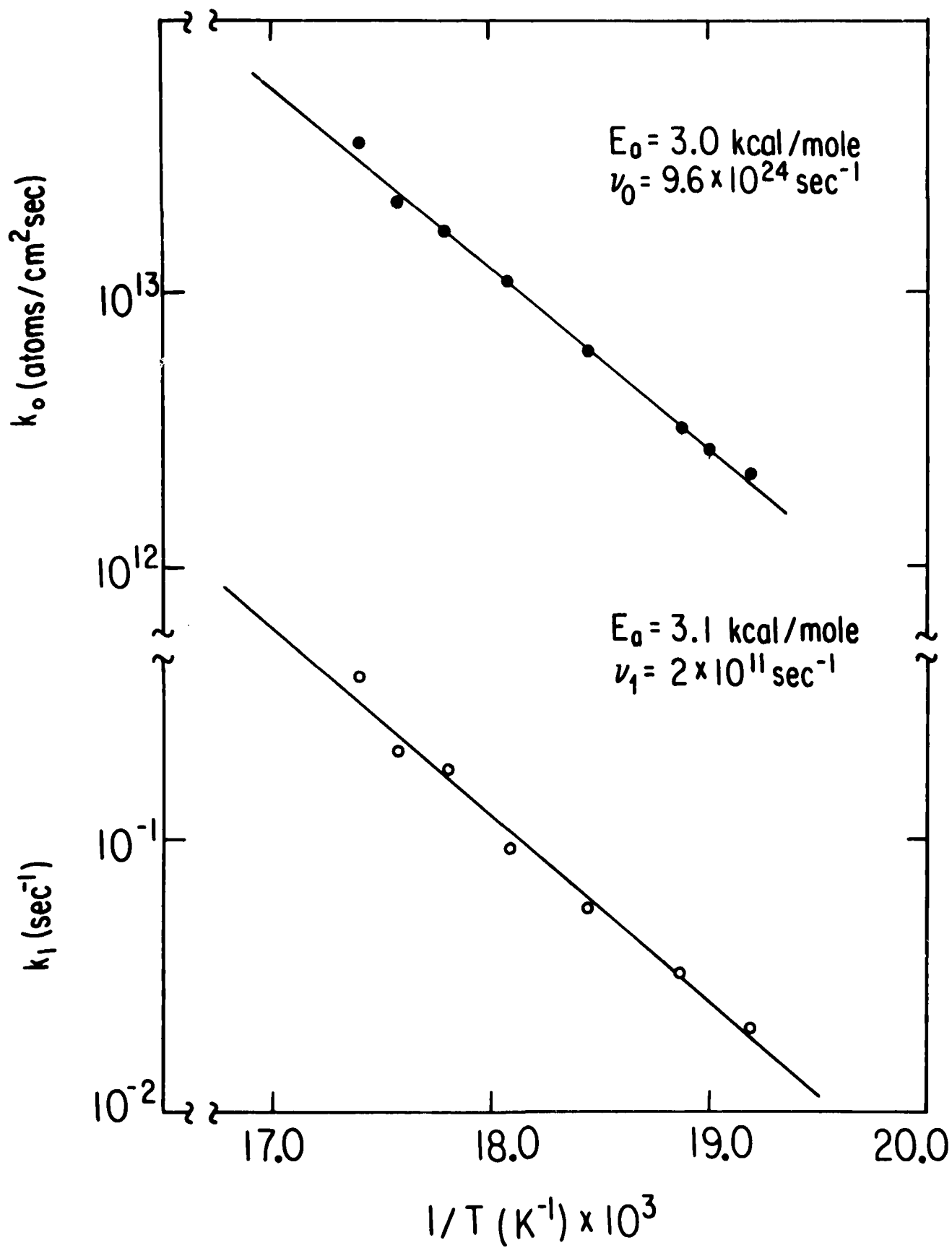


Fig.8

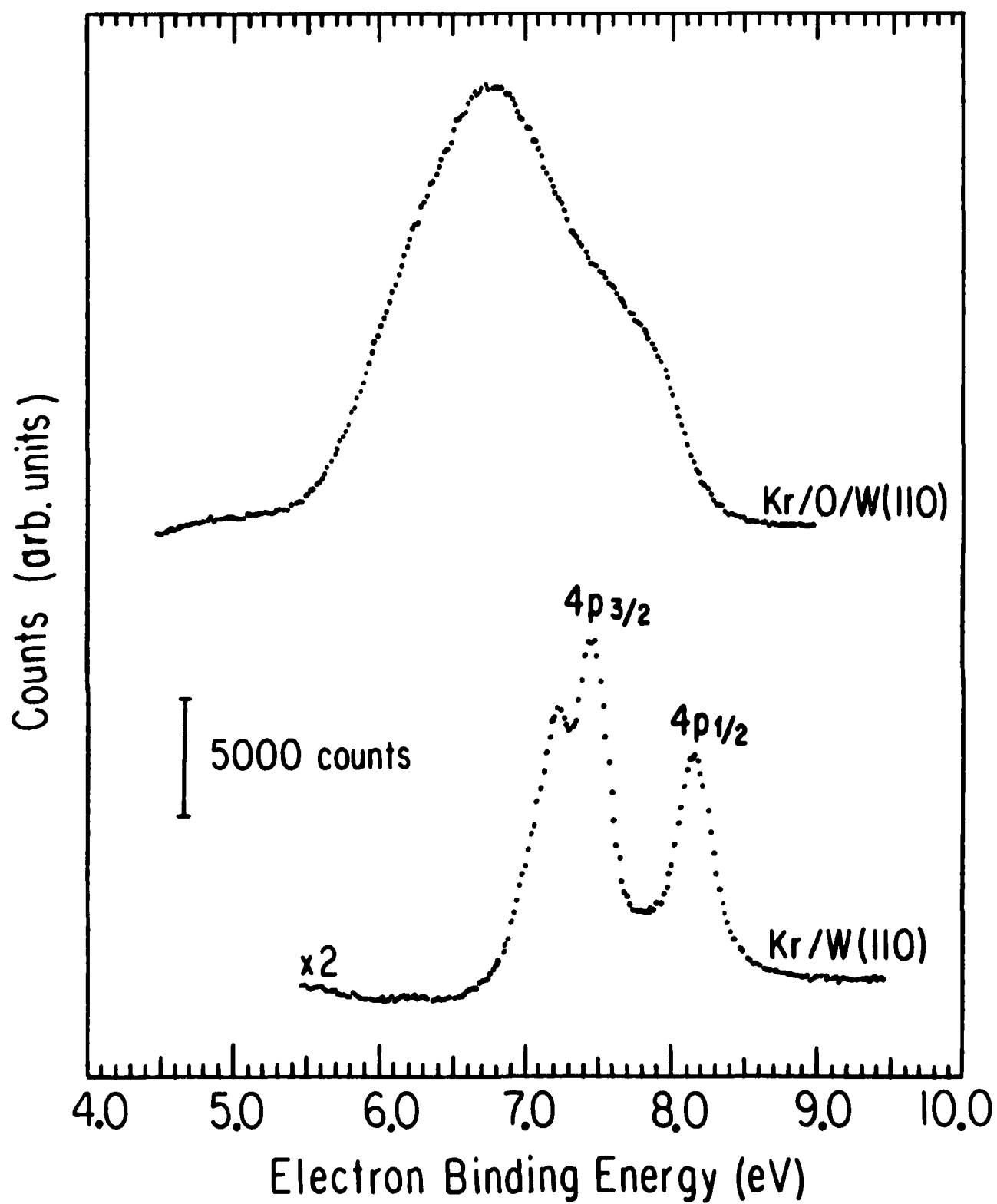


Fig. 9

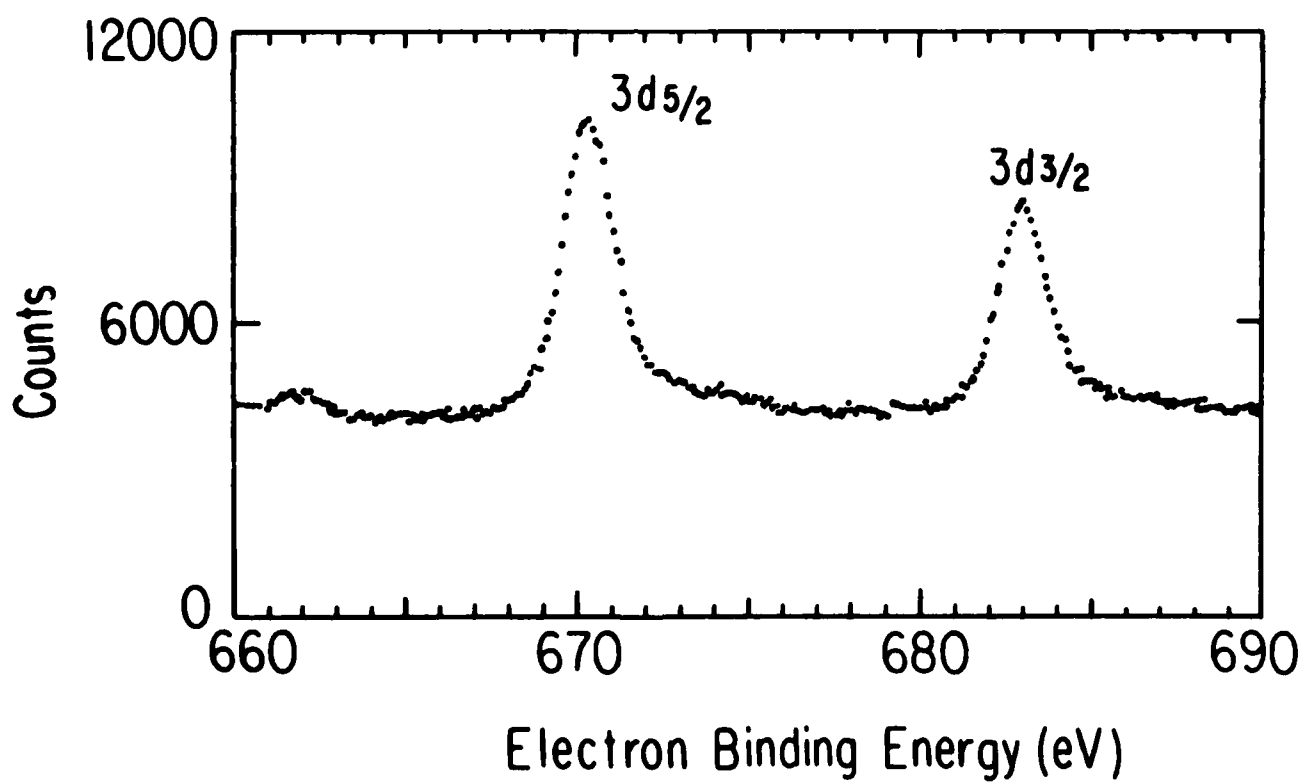
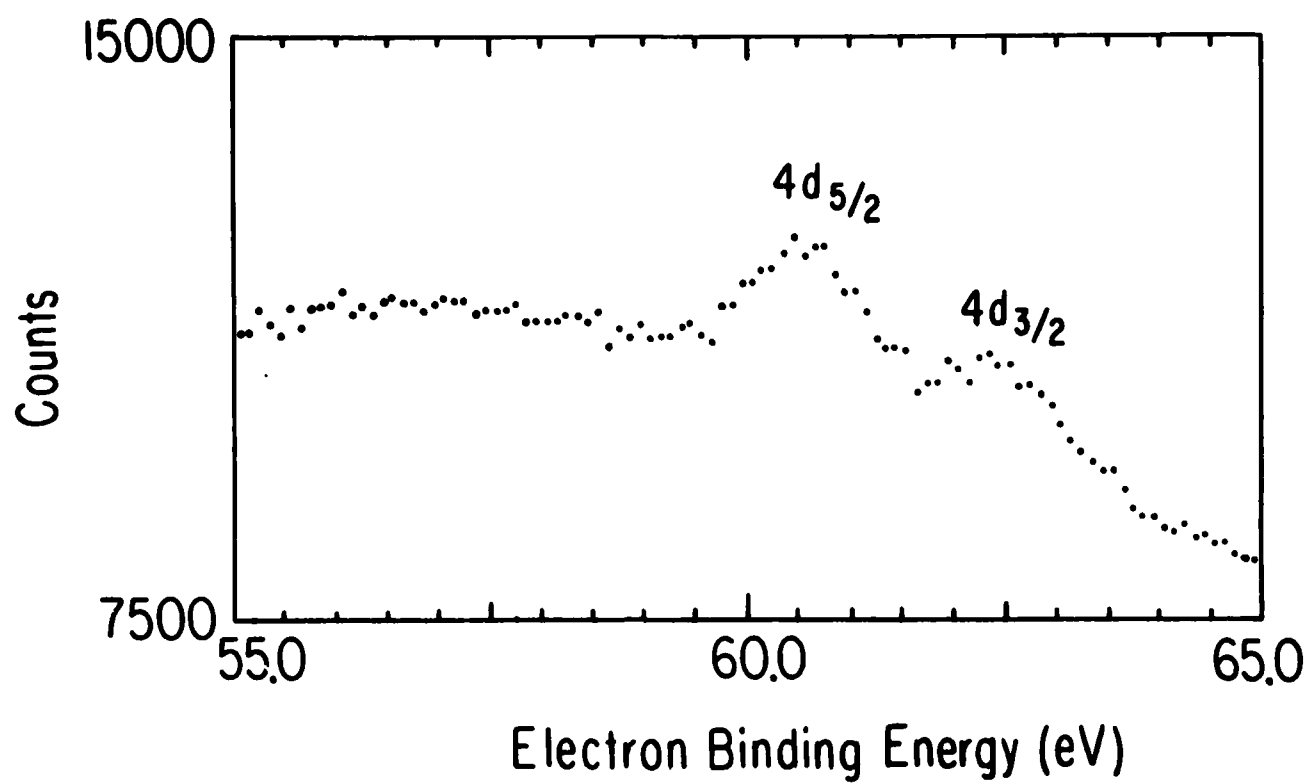


Fig.10

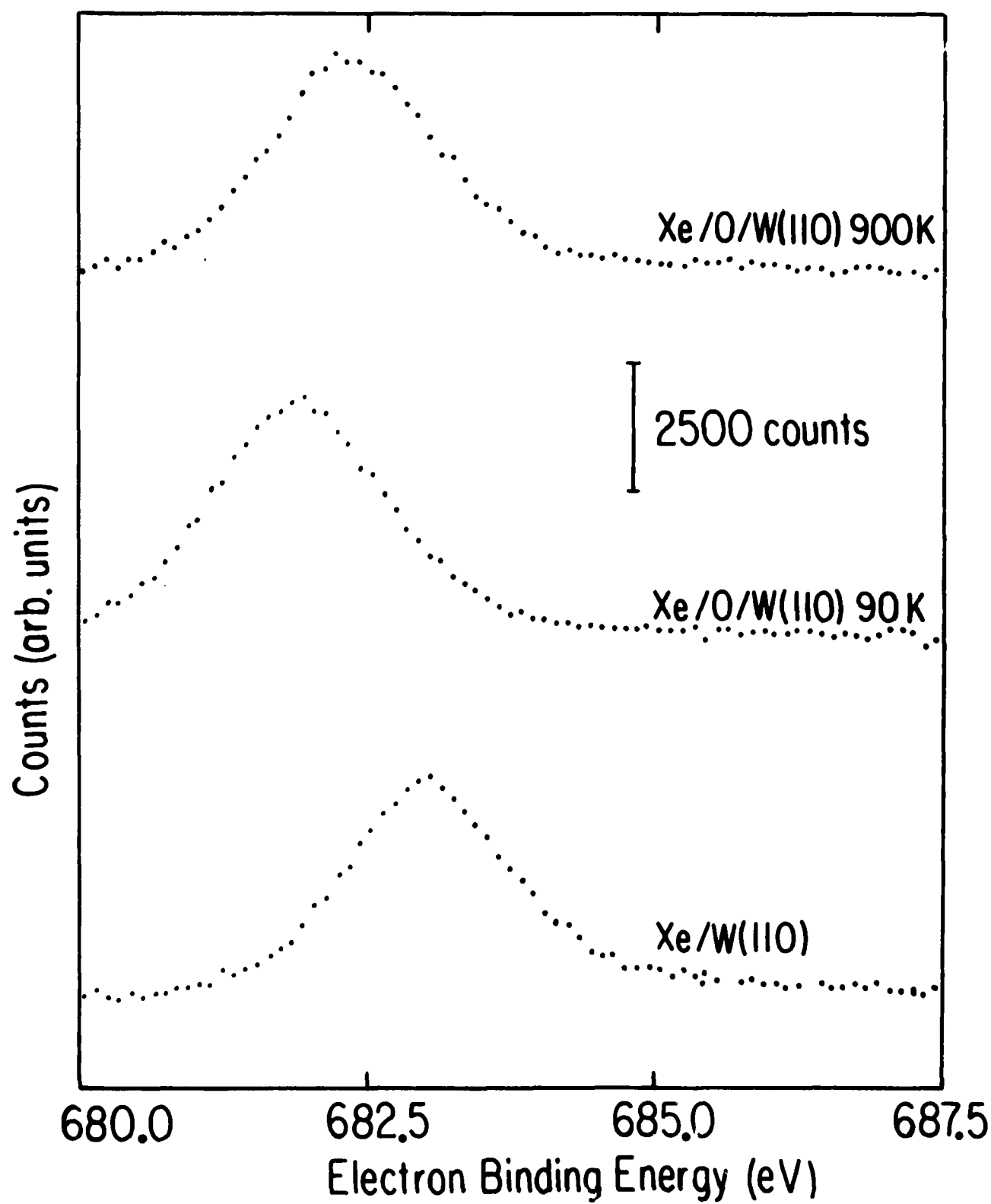


Fig.II

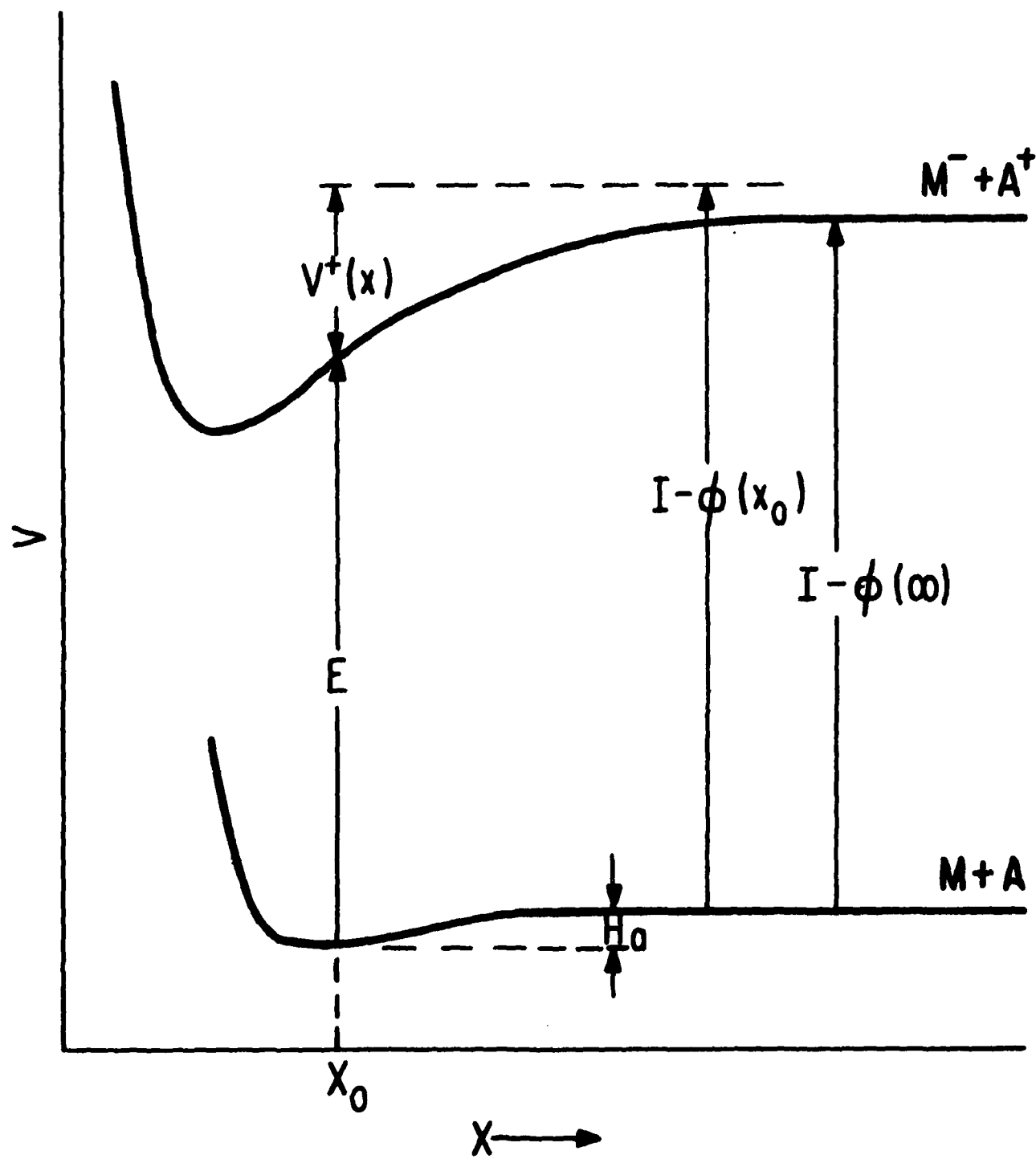


Fig.12

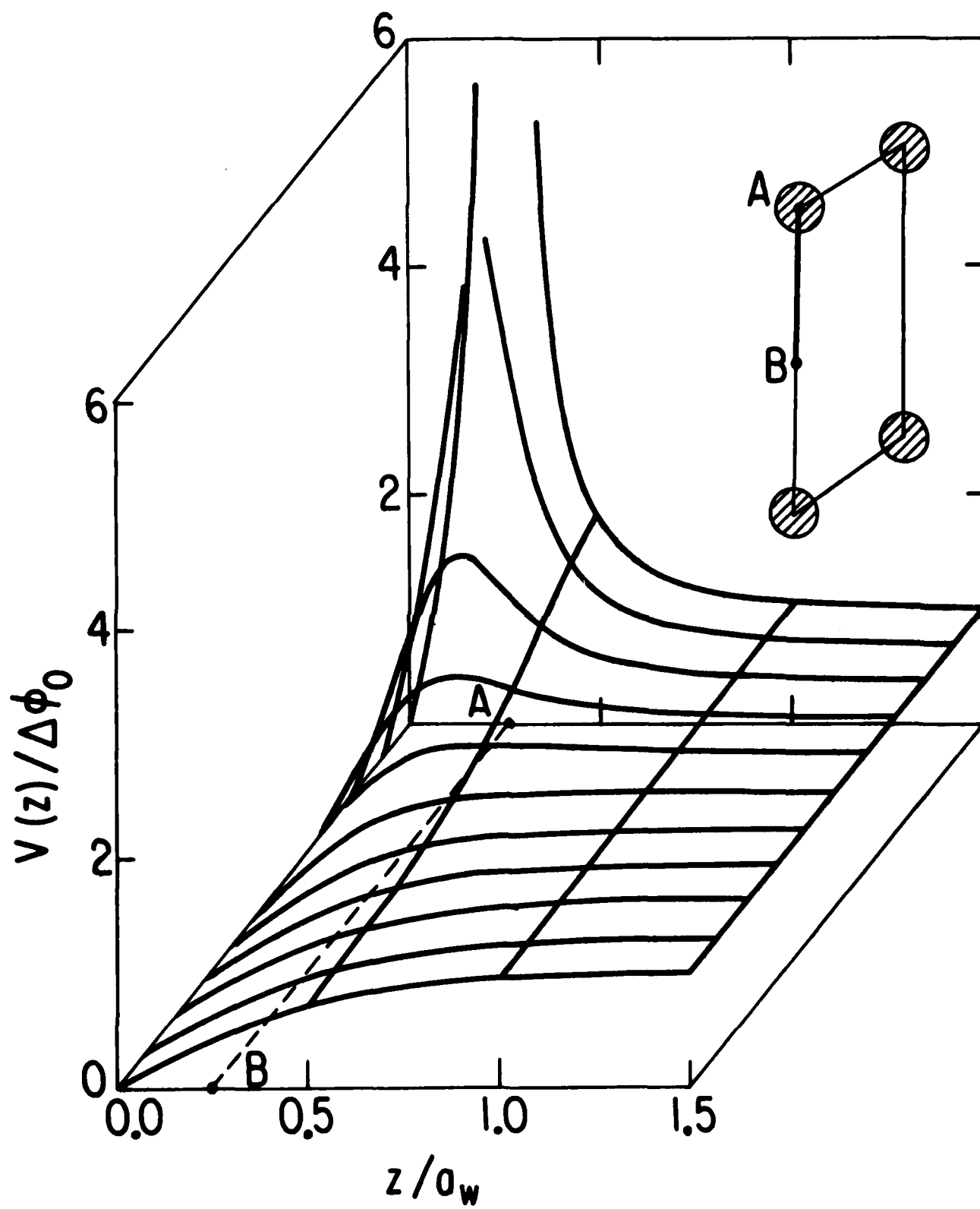
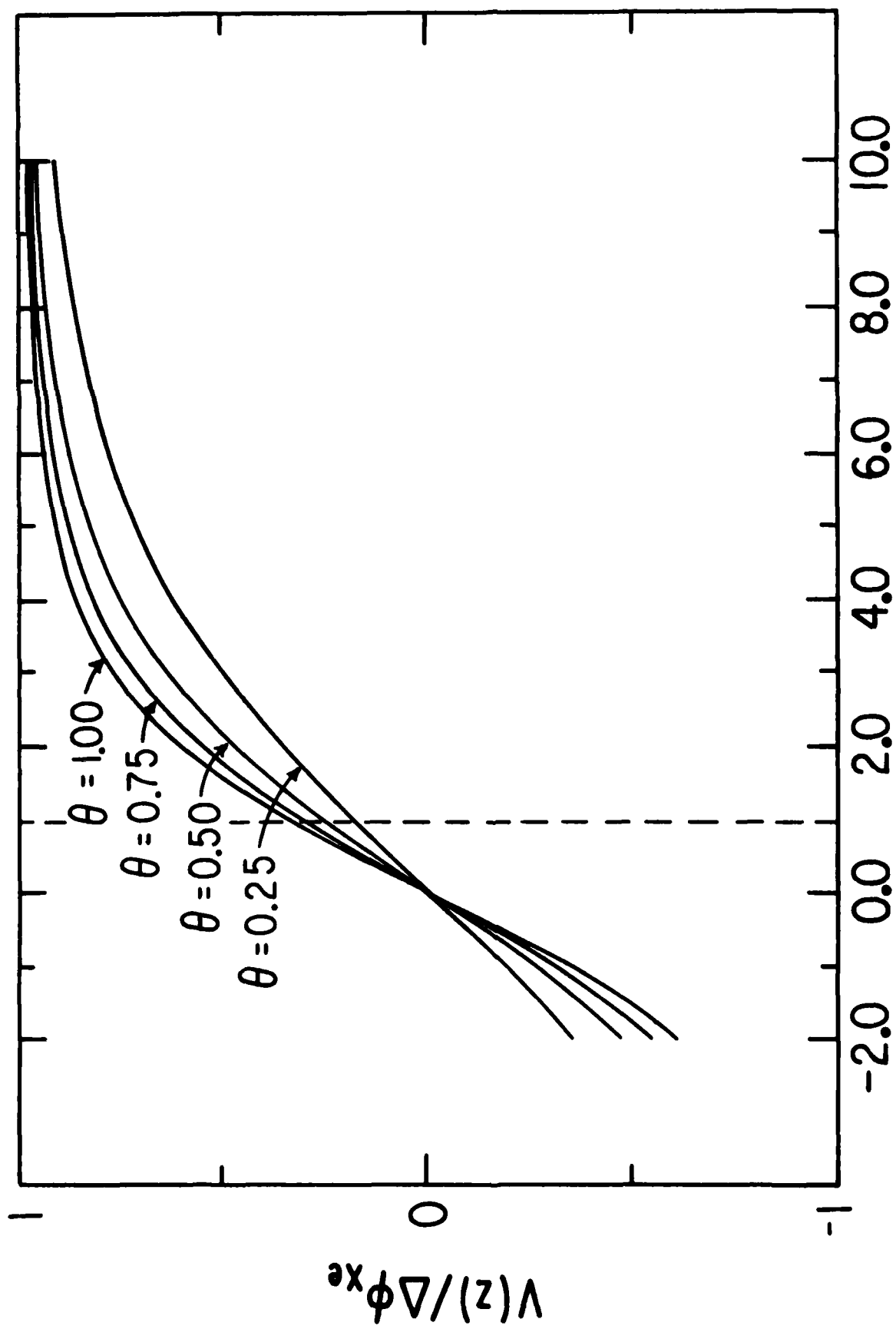


Fig.13



z/r_{xe}

Fig.14

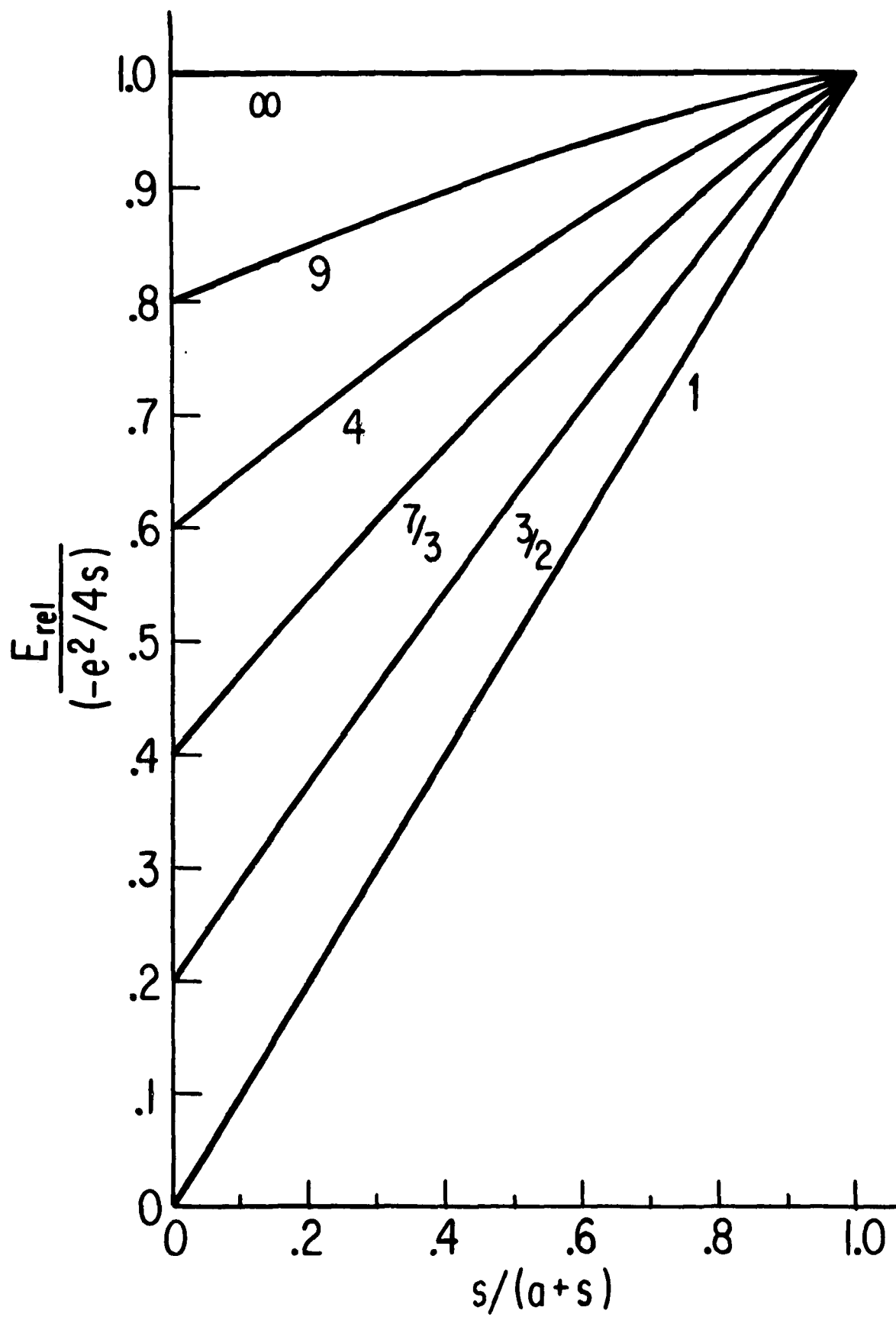


Fig.15

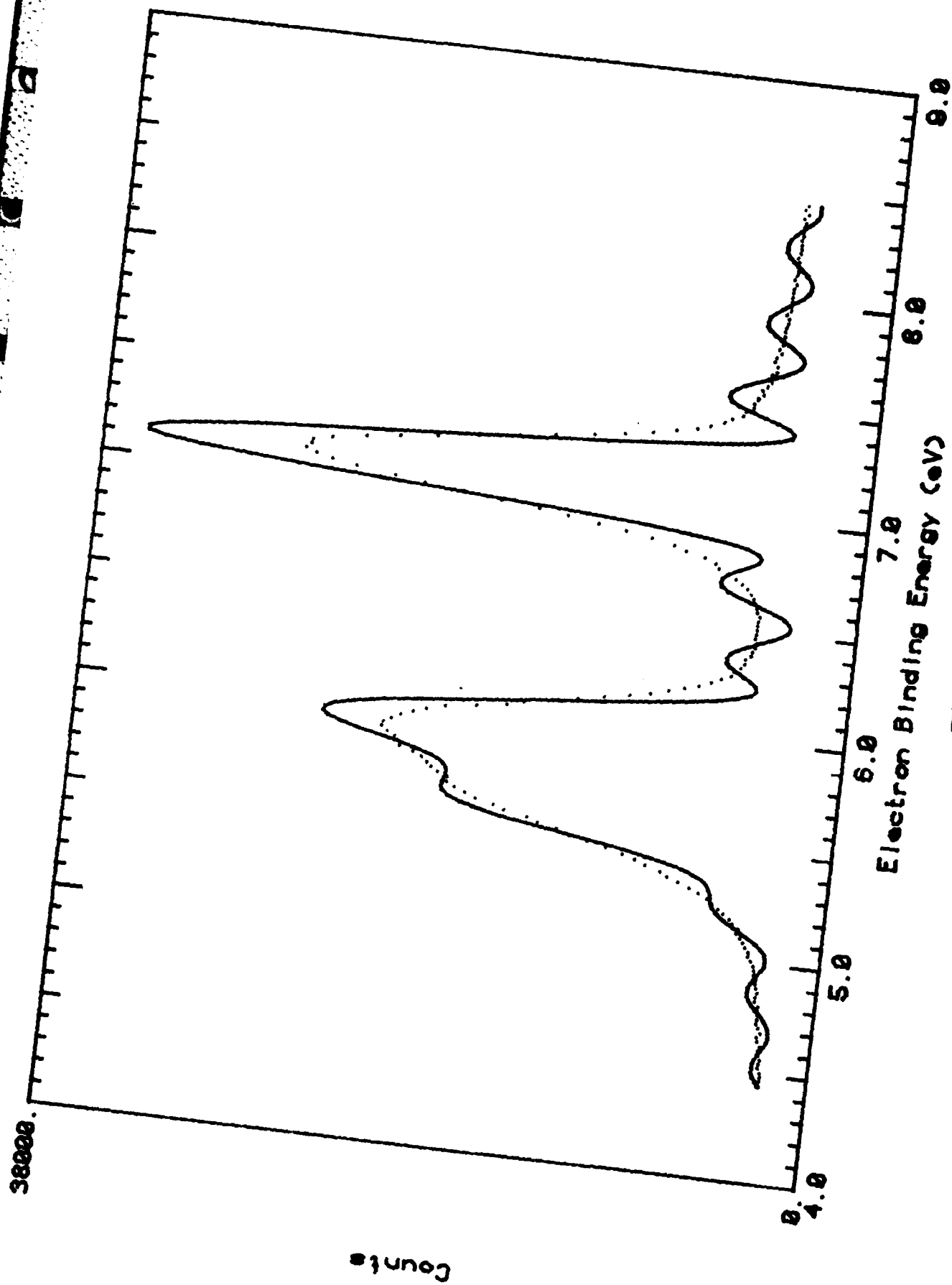


Fig.16

Kr/O/WC(110)

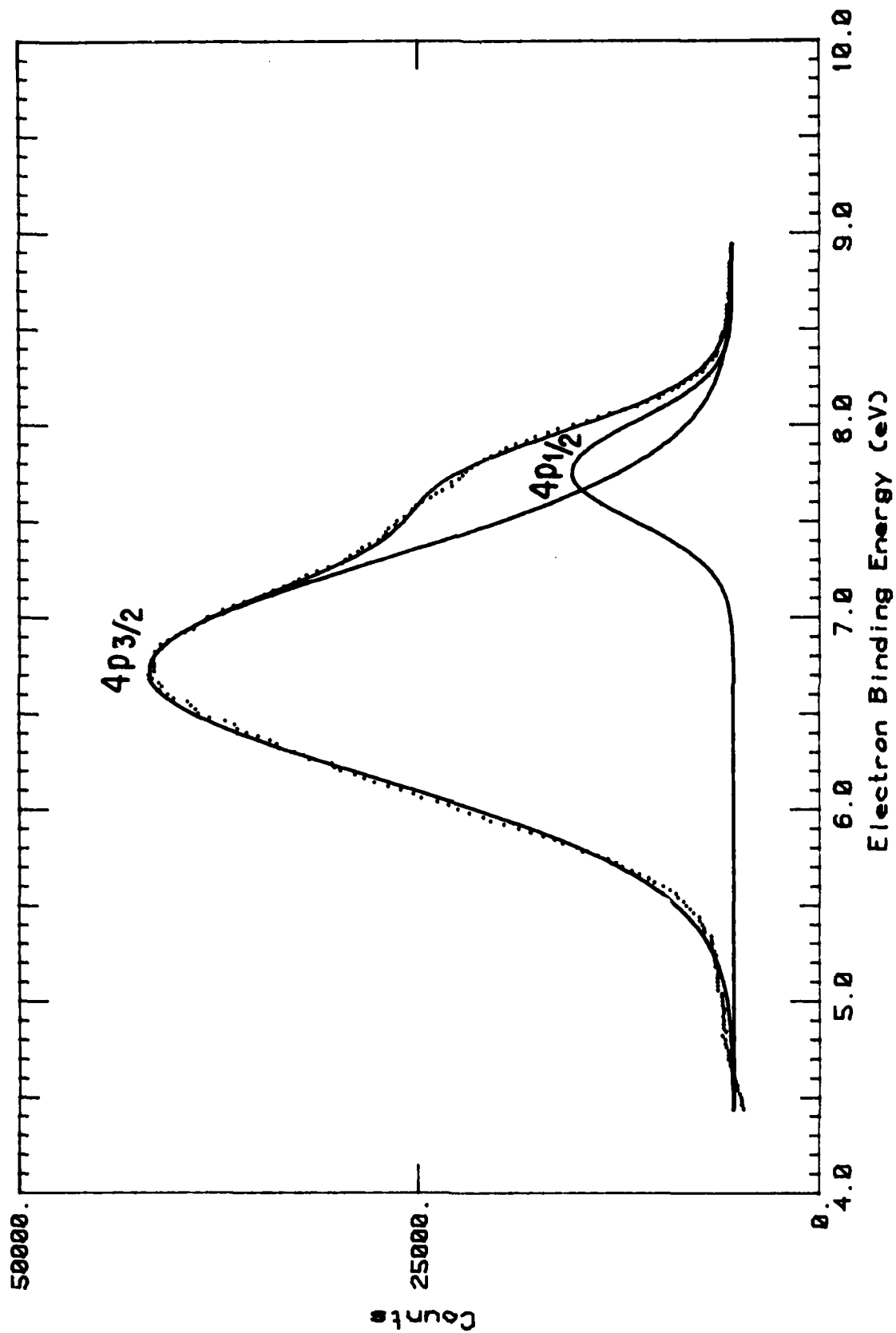


Fig.17

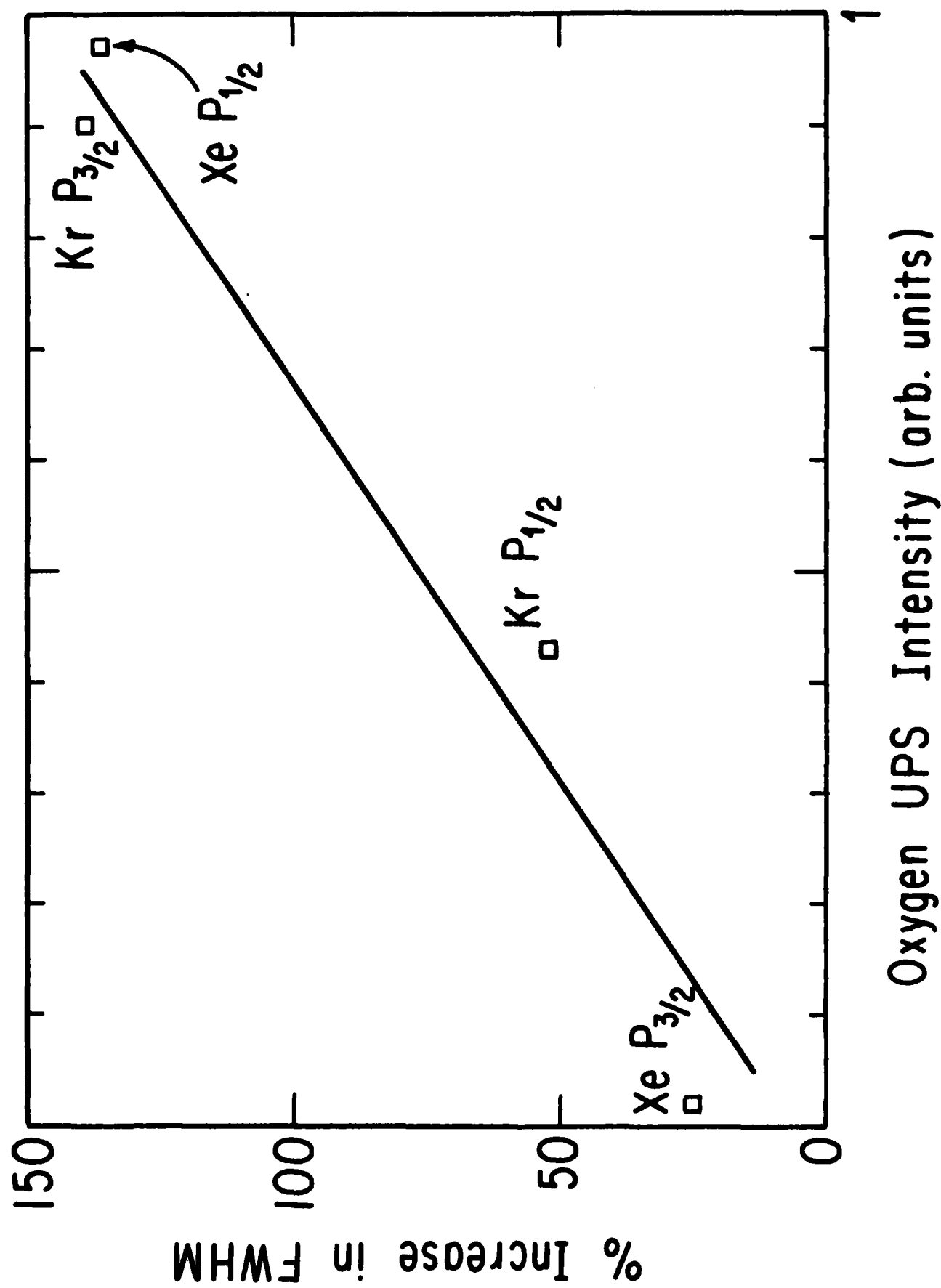


Fig.18

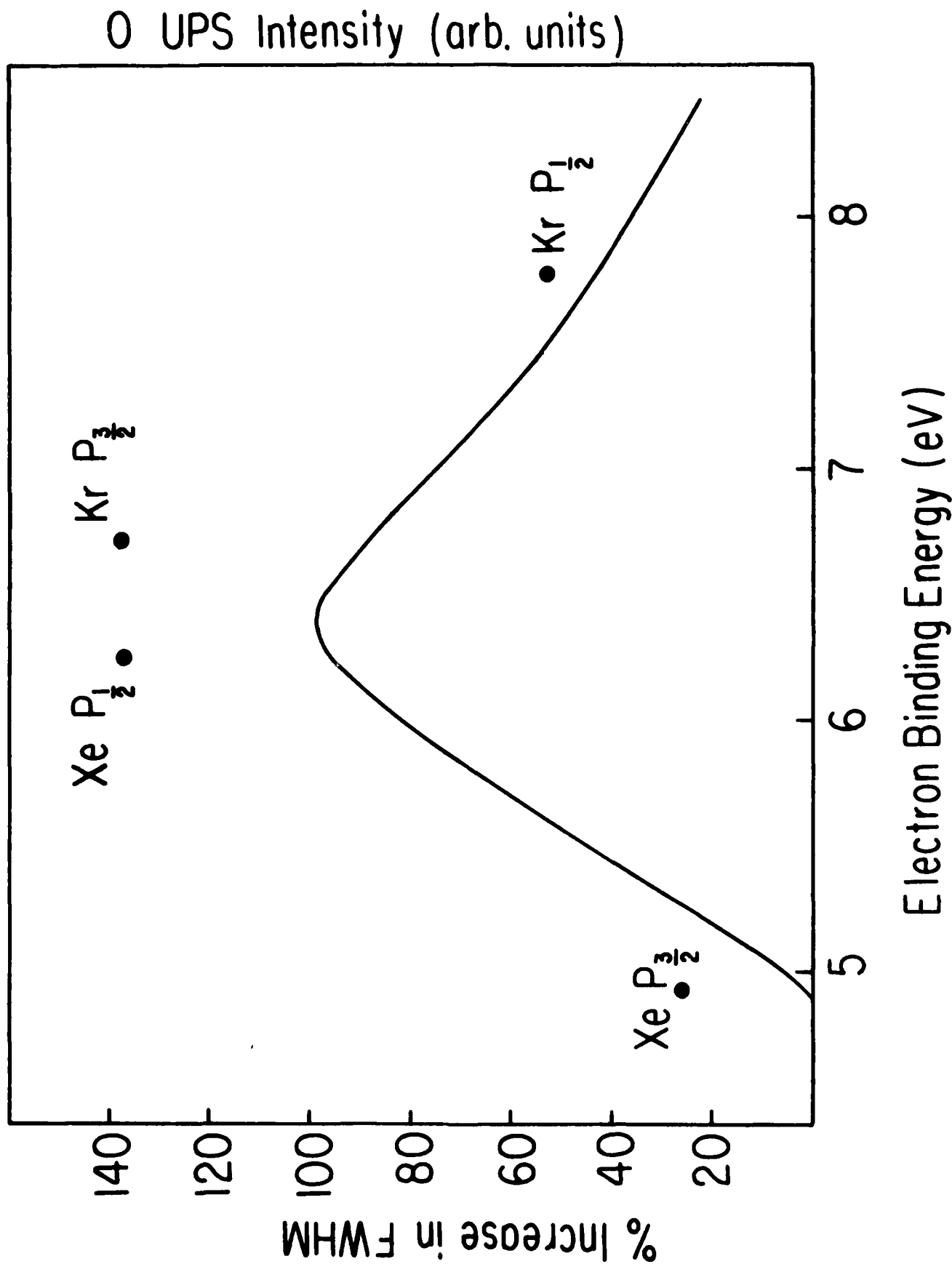


Fig.19

END

FILMED

2-83

DTIC